

The narrow capture problem: an encounter-based approach to partially reactive targets

Paul C. Bressloff

Department of Mathematics, University of Utah 155 South 1400 East, Salt Lake City, UT 84112

A general topic of current interest is the analysis of diffusion problems in singularly perturbed domains with small interior targets or traps (the narrow capture problem). One major application is to intracellular diffusion, where the targets typically represent some form of reactive biochemical substrate. Most studies of the narrow capture problem treat the target boundaries as totally absorbing (Dirichlet), that is, the chemical reaction occurs immediately on first encounter between particle and target surface. In this paper, we analyze the three-dimensional narrow capture problem in the more realistic case of partially reactive target boundaries. We begin by considering classical Robin boundary conditions. Matching inner and outer solutions of the single-particle probability density, we derive an asymptotic expansion of the Laplace transformed flux into each reactive surface in powers of ϵ , where ϵ is the non-dimensionalized target size. In turn, the fluxes determine the splitting probabilities and conditional first passage times (FPTs) for target absorption. We then extend our analysis to more general types of reactive targets by combining matched asymptotic analysis with an encounter-based formulation of diffusion-mediated surface reactions. That is, we derive an asymptotic expansion of the joint probability density for particle position and the so-called boundary local time, which characterizes the amount of time that a Brownian particle spends in the neighborhood of a point on a totally reflecting boundary. The effects of surface reactions are then incorporated via an appropriate stopping condition for the boundary local time. Robin boundary conditions are recovered in the special case of an exponential law for the stopping local times. Finally, we illustrate the theory by exploring how the leading-order contributions to the splitting probabilities and conditional mean FPTs depend on the choice of surface reactions. In particular, we show that there is an effective renormalization of the target radius of the form $\rho \rightarrow \rho - \tilde{\Psi}(1/\rho)$, where $\tilde{\Psi}$ is the Laplace transform of the stopping local time distribution.

I. INTRODUCTION

A topic of increasing interest is the analysis of two-dimensional (2D) and three-dimensional (3D) diffusion in singularly perturbed domains [1–25]. Two broad classes of problem are diffusion in a domain with small interior targets or traps, and diffusion in a domain with an exterior boundary that is reflecting almost everywhere, except for one or more small holes through which particles can escape. One major application of these studies is molecular diffusion within biological cells, where interior targets could represent (possibly reactive) intracellular compartments and holes on the boundary could represent ion channels or nuclear pores [26, 44]. Quantities of interest at the level of bulk diffusion include the steady-state solution (assuming it exists) and the approach to steady state, as characterized by the leading non-zero eigenvalue λ_1 of the negative Laplacian [1–3, 12] or by the so-called accumulation time [25]. In addition, the flux into an interior target can be used to determine an effective reaction rate [4, 17]. At the single-particle level, the solution of the diffusion equation (or more general Fokker-Planck equation) represents the probability density to find the particle at a particular location. One is now typically interested in calculating the splitting probabilities and conditional mean first passage times time for a particle to be captured by an interior target (narrow capture) [8, 13, 15, 16, 20, 21, 23, 24] or to escape from a domain through a small hole in the boundary (narrow escape) [5, 7, 9–11, 14, 18, 19, 22]. For all of

these examples, the quantity of interest satisfies an associated boundary value problem (BVP), which can be solved using a mixture of matched asymptotic analysis and Green’s function methods.

Within the context of narrow capture problems in cell biology, absorption by a target typically represents some form of chemical reaction. In almost all studies of diffusion in singularly perturbed domains, the boundary conditions imposed on the small targets are taken to be totally absorbing (Dirichlet). A totally absorbing target means that the only contribution to the effective reaction rate is the transport process itself, since the chemical reaction occurs immediately on first encounter between particle and target. In other words, the reaction is diffusion-limited rather than reaction-limited [28]. However, a more realistic scenario is to consider a combination of a transport step and a reaction step, both of which contribute to the effective reaction rate. Collins and Kimball [29] incorporated an imperfect reaction on a target surface $\partial\Omega$ by replacing the Dirichlet boundary condition with the Robin or partially reflecting boundary condition

$$-D\nabla c(\mathbf{x}, t) \cdot \mathbf{n} = \kappa_0 c(\mathbf{x}, t), \quad \mathbf{x} \in \partial\Omega.$$

Here $c(\mathbf{x}, t)$ is particle concentration, \mathbf{n} is the unit normal at the boundary that is directed towards the center of the target, D is the diffusivity, and κ_0 (in units m/s) is known as the reactivity constant. The above boundary condition implies that there is a net flux of particles into the target (left-hand side), which is equal to the rate at which par-

ticles react with (are absorbed by) the target (right-hand side). The latter is taken to be proportional to the particle concentration at the target with κ_0 the constant of proportionality. The totally absorbing case is recovered in the limit $\kappa_0 \rightarrow \infty$, whereas the case of an inert (perfectly reflecting) target is obtained by setting $\kappa_0 = 0$. In practice, the diffusion-limited and reaction-limited cases correspond to the regimes $\Lambda \ll R$ and $\Lambda \gg R$, respectively. Here R is a geometric length-scale such as the radius of a spherical target and $\Lambda = D/\kappa_0$ is known as the reaction length. Note that there have been a few studies of bulk diffusion in singularly perturbed domains containing targets with Robin boundary conditions [1–3, 6]. It is also possible to obtain Robin boundary conditions by spatially homogenizing a target with mixed boundary conditions [19], or by considering a stochastically-gated target in an appropriate limit [30]. However, as far as we are aware, there have not been any detailed studies at the single-particle level.

As recently highlighted by Grebenkov [31], the single-particle probabilistic interpretation of the partially reflecting boundary condition is much more complicated than the Dirichlet boundary condition. The latter is easily incorporated into Brownian motion by introducing the notion of a first passage time, which is a particular example of a stopping time. On the other hand, the inclusion of a totally or partially reflecting boundary requires a modification of the stochastic process itself. Mathematically speaking, one can construct so-called reflected Brownian motion in terms of a boundary local time, which characterizes the amount of time that a Brownian particle spends in the neighborhood of a point on a totally reflecting boundary [32, 33]. The resulting stochastic differential equation, also known as the stochastic Skorokhod equation [34], can then be extended to take into account chemical reactions, thus providing a probabilistic implementation of the Robin boundary condition [35, 36]. A simpler conceptual framework for understanding partially reflected Brownian motion is to model diffusion as a discrete-time random walk on a hypercubic lattice \mathbb{Z}^d with lattice spacing a . At a bulk site, a particle jumps to one of the neighboring sites with probability $1/2d$, whereas at a boundary site, it either reacts with probability $q = (1 + \Lambda/a)^{-1}$ or return to a neighboring bulk site with probability $1 - q$. Since the random jumps are independent of the reaction events, it follows that the random number of jumps \hat{N} before a reaction occurs is given by a geometric distribution: $\mathbb{P}[\hat{N} = n] = q(1 - q)^n$, integer $n \geq 0$. In particular, $\mathbb{E}[\hat{N}] = (1 - q)/q = \Lambda/a$. Introducing the rescaled random variable $\hat{\ell} = a\hat{N}$, one finds that [31, 37]

$$\begin{aligned} \mathbb{P}[\hat{\ell} \geq \ell] &= \mathbb{P}[\hat{N} \geq \ell/a] = (1 - q)^{\ell/a} = (1 + a/\Lambda)^{-\ell/a} \\ &\xrightarrow[a \rightarrow 0]{} e^{-\ell/\Lambda}. \end{aligned}$$

That is, for sufficiently small lattice spacing a , a reaction occurs (the random walk is terminated) when the random number of realized jumps from boundary sites, multiplied

by a , exceeds an exponentially distributed random variable (stopping local time) $\hat{\ell}$ with mean Λ . Assuming that a partially reflected random walk on a lattice converges to a well-defined continuous process in the limit $a \rightarrow 0$ (see Refs. [35, 36]), one can define partially reflected Brownian motion as reflected Brownian motion stopped at the random time [31, 38, 39]

$$\mathcal{T} = \inf\{t > 0 : \ell_t > \hat{\ell}\},$$

where ℓ_t is the local time of the reflected Brownian motion. The latter is the continuous analog of the rescaled number of surface encounters $(a\hat{N})$, and $\mathbb{P}[\hat{\ell} > \ell] = e^{-\ell/\Lambda}$. The reaction length Λ thus parameterizes the stochastic process. (Note that it is also possible to construct more general partially reflecting diffusion processes by considering the continuous limit of more general Markovian jump processes [40].)

One major advantage of the above formulation of partially reflected Brownian motion is that it provides a theoretical framework for investigating more general diffusion-mediated surface phenomena [41–43]. In particular, by considering the joint probability density $P(\mathbf{x}, \ell, t)$ for the pair (\mathbf{X}_t, ℓ_t) , where \mathbf{X}_t is the particle position at time t and ℓ_t is the boundary local time, one can analyze the bulk dynamics in a domain with perfectly reflecting boundaries and then incorporate the effects of surface reactions via an appropriate stopping condition for the boundary local time. In particular, the probability density $p(\mathbf{x}, t)$ for partially reflected Brownian motion can be expressed as the Laplace transform of a propagator P :

$$p(\mathbf{x}, t) = \int_0^\infty e^{-\ell/\Lambda} P(\mathbf{x}, \ell, t) d\ell,$$

where Λ is the previously defined reaction length. This so-called encounter-based approach allows one to go beyond the case of constant reactivity (Robin boundary conditions) by considering more general probability distributions $\Psi(\ell) = \mathbb{P}[\hat{\ell} > \ell]$ for the stopping local time $\hat{\ell}$ and setting [41–43]

$$p(\mathbf{x}, t) = \int_0^\infty \Psi(\ell) P(\mathbf{x}, \ell, t) d\ell.$$

For example, reaction rates could depend on the number of encounters between the particle and surface. The separation of the bulk dynamics from surface reactions means that all of the geometrical aspects of the diffusion process are disentangled from the reaction kinetics. Geometrical features include the structure of both reactive and non-reactive surfaces. Returning to the narrow capture problem, the exterior boundary of the domain would correspond to a non-reactive surface, say, while the reactive surfaces would be given by the interior target boundaries. In the case of small targets, matched asymptotic methods provide a way of further separating geometrical effects. That is, the bulk dynamics is partitioned into

an outer solution that depends on the exterior boundary and an inner solution that depends on the geometry of the targets.

In this paper, we analyze the 3D narrow capture problem for small spherical targets with partially reactive boundary surfaces. We proceed by combining the encounter-based approach to diffusion-mediated surface reactions [41–43] with matched asymptotic methods [24]. We begin by considering the narrow capture problem for reactive surfaces with classical Robin boundary conditions, see Sect. II. Working in Laplace space, we construct an inner solution around each target, and then match it with an outer solution in the bulk. This yields an asymptotic expansion of the Laplace transformed flux into each reactive surface in powers of ϵ , where ϵ is the non-dimensionalized target size. The Laplace transformed fluxes are then used to determine the splitting probabilities and mean first passage times (MFPTs) in the small- s limit, where s is the Laplace variable. As previously highlighted in Ref. [24], the small- s limit is non-trivial due to the fact that the corresponding Laplace transformed Green's function has a singularity of the form $G(\mathbf{x}, s|\mathbf{x}_0) \sim 1/s$. The resulting singularities in the asymptotic expansion of the Laplace transformed flux into each target can be eliminated by considering a triple expansion in ϵ , s and $\Gamma \propto \epsilon/s$. Performing partial summations over infinite power series in Γ leads to multiplicative factors of the form $\Gamma^n/(1 + \Gamma)^n$. Since $\Gamma^n/(1 + \Gamma)^n \rightarrow 1$ as $s \rightarrow 0$, the singularities in s are removed. We thus obtain Λ -dependent expressions for the splitting probabilities and MFPTs, which recover previous results for totally absorbing targets in the limit $\Lambda = D/\kappa_0 \rightarrow 0$.

In Sect. III we briefly summarize the encounter-based formulation of diffusion-mediated surface reactions developed in Ref. [42]. In particular, we define the boundary local time ℓ_t for diffusion in a domain Ω with a perfectly reflecting boundary $\partial\Omega$ and write down the BVP for the associated propagator. It turns out that for the narrow capture problem, it is more convenient to work directly with the BVP rather than using the spectral decomposition of the propagator and the so-called Dirichlet-to-Neumann operator [31, 41, 42]. In Sect. IV we use matched asymptotics to analyze the corresponding propagator BVP for the narrow escape problem, in which the reactive boundaries of the interior targets are replaced by totally reflecting boundaries. This then allows us to incorporate generalized surface reactions by considering an appropriately defined distribution $\Psi(\ell)$ of stopping local times. We thus obtain an asymptotic expansion of the inner solution for the Laplace transformed probability density and the corresponding target fluxes. We also show that our results for Robin boundary conditions in Sect. II are recovered in the special case $\Psi(\ell) = e^{-\ell/\Lambda}$. Finally, we illustrate the theory in Sect. V by exploring how the leading-order contributions to the splitting probabilities and conditional MFPTs depend on the choice of surface reactions. In particular, we show that there is an

effective renormalization of the target radius of the form $\rho \rightarrow \rho - \tilde{\Psi}(1/\rho)$, where $\tilde{\Psi}$ is the Laplace transform of the stopping local time distribution.

II. NARROW CAPTURE PROBLEM: ROBIN BOUNDARY CONDITIONS

Consider a 3D bounded domain $\Omega \subset \mathbb{R}^3$ that contains a set of N small, interior, partially absorbing targets \mathcal{U}_k , $k = 1, \dots, N$, see Fig. 1. Each target is assumed to have a volume $|\mathcal{U}_j| \sim \epsilon^3 |\Omega|$ with $\mathcal{U}_j \rightarrow \mathbf{x}_j \in \Omega$ uniformly as $\epsilon \rightarrow 0$, $j = 1, \dots, N$. The targets are also taken to be well separated in the sense that $|\mathbf{x}_i - \mathbf{x}_j| = O(1)$, $j \neq i$, and $\text{dist}(\mathbf{x}_j, \partial\Omega) = O(1)$. For concreteness we will take each target to be a sphere of radius $\epsilon\rho_j$. Thus $\mathcal{U}_i = \{\mathbf{x} \in \Omega, |\mathbf{x} - \mathbf{x}_i| \leq \epsilon\rho_i\}$. Let $p(\mathbf{x}, t|\mathbf{x}_0)$ be the probability density that at time t a particle is at $\mathbf{X}(t) = \mathbf{x}$, having started at position \mathbf{x}_0 . Setting $\bigcup_{j=1}^N \mathcal{U}_j = \mathcal{U}_a \subset \Omega$, we have

$$\frac{\partial p(\mathbf{x}, t|\mathbf{x}_0)}{\partial t} = D\nabla^2 p(\mathbf{x}, t|\mathbf{x}_0), \quad \mathbf{x} \in \Omega \setminus \mathcal{U}_a, \quad (2.1a)$$

$$\nabla p \cdot \mathbf{n} = 0, \quad \mathbf{x} \in \partial\Omega, \quad (2.1b)$$

$$D\nabla p(\mathbf{x}, t|\mathbf{x}_0) \cdot \mathbf{n}_k = -\kappa_0 p(\mathbf{x}, t|\mathbf{x}_0), \quad \mathbf{x} \in \partial\mathcal{U}_k, \quad (2.1c)$$

together with the initial condition $p(\mathbf{x}, t|\mathbf{x}_0) = \delta(\mathbf{x} - \mathbf{x}_0)$. Here \mathbf{n} and \mathbf{n}_k are the outward unit normals to the surfaces $\partial\Omega$ and $\partial\mathcal{U}_k$, respectively. Eq. (2.1b) is a Robin boundary condition with the constant reactivity parameter κ_0 having units m/s [29]. Dirichlet and Neumann boundary conditions are recovered in the limits $\kappa_0 \rightarrow \infty$ and $\kappa_0 \rightarrow 0$, respectively.

A. Matched asymptotics

In order to calculate various quantities of interest such as splitting probabilities and conditional first passage times, it is more convenient to work in Laplace space:

$$D\nabla^2 \tilde{p}(\mathbf{x}, s|\mathbf{x}_0) - s\tilde{p}(\mathbf{x}, s|\mathbf{x}_0) = -\delta(\mathbf{x} - \mathbf{x}_0), \quad \mathbf{x} \in \Omega \setminus \mathcal{U}_a, \quad (2.2a)$$

$$D\nabla \tilde{p} \cdot \mathbf{n} = 0, \quad \mathbf{x} \in \partial\Omega \quad (2.2b)$$

$$D\nabla \tilde{p}(\mathbf{x}, s|\mathbf{x}_0) \cdot \mathbf{n}_k = -\kappa_0 \tilde{p}(\mathbf{x}, s|\mathbf{x}_0), \quad \mathbf{x} \in \partial\mathcal{U}_k. \quad (2.2c)$$

Eqs. (2.2) define a boundary value problem that can be analyzed along analogous lines to previous studies of diffusion in 3D domains with small targets [12, 16, 24]. We proceed by matching appropriate ‘inner’ and ‘outer’ asymptotic expansions in the limit of small target size $\epsilon \rightarrow 0$, see Figs. 1(b,c).

In the outer region, $\tilde{p}(\mathbf{x}, s|\mathbf{x}_0)$ is expanded as

$$\tilde{p}(\mathbf{x}, s|\mathbf{x}_0) \sim \tilde{p}_0(\mathbf{x}, s|\mathbf{x}_0) + \epsilon \tilde{p}_1(\mathbf{x}, s|\mathbf{x}_0) + \epsilon^2 \tilde{p}_2(\mathbf{x}, s|\mathbf{x}_0) + \dots$$

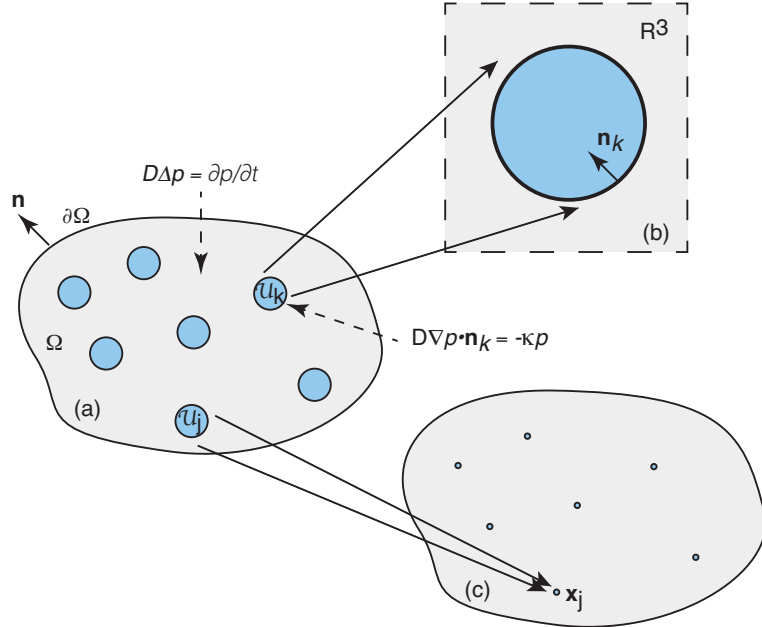


FIG. 1. Brownian particle in a singularly perturbed domain. (a) Particle diffuses in a bounded domain Ω containing N small interior targets denoted by \mathcal{U}_j , $j = 1, \dots, N$. The exterior boundary $\partial\Omega$ is reflecting, whereas the j -th interior boundary $\partial\mathcal{U}_i$ is partially absorbing. (b) Construction of the inner solution in terms of stretched coordinates $\mathbf{y} = \epsilon^{-1}(\mathbf{x} - \mathbf{x}_i)$, where \mathbf{x}_i is the center of the i -th target. The rescaled radius is ρ_i and the region outside the target is taken to be \mathbb{R}^3 rather than the bounded domain Ω . (c) Construction of the outer solution. Each target is shrunk to a single point. The outer solution can be expressed in terms of the corresponding modified Neumann Green's function and then matched with the inner solution around each target.

The leading order term is the solution without any holes and satisfies

$$D\nabla^2\tilde{p}_0 - s\tilde{p}_0 = -\delta(\mathbf{x} - \mathbf{x}_0), \quad \mathbf{x} \in \Omega, \quad (2.3a)$$

$$\nabla\tilde{p}_0 \cdot \mathbf{n} = 0, \quad \mathbf{x} \in \partial\Omega. \quad (2.3b)$$

That is, $\tilde{p}_0 = G(\mathbf{x}, s|\mathbf{x}_0)$ where G is the Neumann Green's function of the modified Helmholtz equation. In particular,

$$\int_{\Omega} G(\mathbf{x}, s|\mathbf{x}_0) d\mathbf{x} = \frac{1}{s}, \quad (2.4a)$$

$$G(\mathbf{x}, s|\mathbf{x}_0) = \frac{1}{4\pi D|\mathbf{x} - \mathbf{x}_0|} + R(\mathbf{x}, s|\mathbf{x}_0), \quad (2.4b)$$

where R is the regular part of G . On the other hand, for $m \geq 1$, we have to solve the equation

$$D\nabla^2\tilde{p}_m - s\tilde{p}_m = 0, \quad \mathbf{x} \in \Omega \setminus \{\mathbf{x}_1, \dots, \mathbf{x}_N\} \quad (2.5a)$$

$$\nabla\tilde{p}_m \cdot \mathbf{n} = 0, \quad \mathbf{x} \in \partial\Omega, \quad (2.5b)$$

together with certain singularity conditions as $\mathbf{x} \rightarrow \mathbf{x}_j$, $j = 1, \dots, N$. The latter are determined by matching to the inner solution.

Next we introduce stretched coordinates $\mathbf{y} = \epsilon^{-1}(\mathbf{x} - \mathbf{x}_j)$ around the j th target and take $\tilde{q}(\mathbf{y}, s|\mathbf{x}_0) = \tilde{p}(\mathbf{x}, s|\mathbf{x}_0)$ to be the corresponding inner solution. Eq. (2.2) implies that

$$D\nabla_{\mathbf{y}}^2\tilde{q}(\mathbf{y}, s|\mathbf{x}_0) - s\epsilon^2\tilde{q}(\mathbf{y}, s|\mathbf{x}_0) = 0, \quad |\mathbf{y}| > \rho_j, \quad (2.6a)$$

$$D\nabla_{\mathbf{y}}\tilde{q}(\mathbf{y}, s|\mathbf{x}_0) \cdot \mathbf{n}_j = -\epsilon\kappa_0\tilde{q}(\mathbf{y}, s|\mathbf{x}_0) \quad |\mathbf{y}| = \rho_j. \quad (2.6b)$$

The details of the analysis of the inner solution will now depend on how the reaction length $\Lambda = D/\kappa_0$ compares to the typical target size $\epsilon\bar{\rho}$, where $\bar{\rho} = N^{-1} \sum_{i=1}^N \rho_j$ for example [3]. We will focus on the regime $\Lambda \sim \epsilon\bar{\rho}$ by rescaling the reactivity according to $\kappa_0 \rightarrow \kappa_0/\epsilon$. (Under this choice of scaling, we can recover the totally absorbing case by taking $\kappa_0 \rightarrow \infty$, that is, $\Lambda \rightarrow 0$. However, the totally reflecting case $\kappa_0 \rightarrow 0$ is inaccessible.) Introducing a perturbation expansion of the inner solution around the j -th target of the form

$$\tilde{q} \sim \tilde{q}_0 + \epsilon\tilde{q}_1 + \epsilon^2\tilde{q}_2 + O(\epsilon^3) \quad (2.7)$$

then yields the following hierarchy of equations (assuming $s \ll 1/\epsilon$)

$$D\nabla_{\mathbf{y}}^2\tilde{q}_m(\mathbf{y}, s|\mathbf{x}_0) = 0, \quad |\mathbf{y}| > \rho_j, \quad m = 0, 1, \quad (2.8a)$$

$$D\nabla_{\mathbf{y}}^2\tilde{q}_m(\mathbf{y}, s|\mathbf{x}_0) = s\epsilon^2\tilde{q}_{m-2}(\mathbf{y}, s|\mathbf{x}_0) = 0, \quad m \geq 2 \quad (2.8b)$$

$$D\nabla_{\mathbf{y}}\tilde{q}_m(\mathbf{y}, s|\mathbf{x}_0) \cdot \mathbf{n}_j = -\kappa_0\tilde{q}_m(\mathbf{y}, s|\mathbf{x}_0) \quad |\mathbf{y}| = \rho_j. \quad (2.8c)$$

These are supplemented by far-field conditions obtained by matching with the near-field behavior of the outer solution. In order to perform the matching, it is necessary to consider the Taylor expansion of G near the j -th target:

$$\begin{aligned} \tilde{p}_0 \sim & G(\mathbf{x}_j, s|\mathbf{x}_0) + \nabla_{\mathbf{x}}G(\mathbf{x}, s|\mathbf{x}_0)|_{\mathbf{x}=\mathbf{x}_j} \cdot (\mathbf{x} - \mathbf{x}_j) \\ & + \frac{1}{2}\mathbf{H}_j \cdot (\mathbf{x} - \mathbf{x}_j) \otimes (\mathbf{x} - \mathbf{x}_j) + \dots, \end{aligned} \quad (2.9)$$

where \mathbf{H}_j is the Hessian

$$H_j^{ab} = \frac{\partial^2}{\partial x_a \partial x_b} G(\mathbf{x}, s|\mathbf{x}_0) \Big|_{\mathbf{x}=\mathbf{x}_j}, \quad a, b \in \{1, 2, 3\}. \quad (2.10)$$

In stretched coordinates this becomes

$$\tilde{p}_0 \sim G(\mathbf{x}_j, s|\mathbf{x}_0) + \epsilon \nabla_{\mathbf{x}} G(\mathbf{x}_j, s|\mathbf{x}_0) \cdot \mathbf{y} + \frac{\epsilon^2}{2} \mathbf{H}_j \cdot \mathbf{y} \otimes \mathbf{y} + \dots \quad (2.11)$$

Let us begin with the leading order contribution to the inner solution. Matching the far-field behavior of \tilde{q}_0 with the near-field behavior of \tilde{p}_0 shows that

$$\nabla_{\mathbf{y}}^2 \tilde{q}_0(\mathbf{y}, s|\mathbf{x}_0) = 0, \quad |\mathbf{y}| > 1, \quad (2.12a)$$

$$\tilde{q}_0 \sim G(\mathbf{x}_j, s|\mathbf{x}_0) \text{ as } |\mathbf{y}| \rightarrow \infty; \quad (2.12b)$$

$$D \nabla_{\mathbf{y}} \tilde{q}_0(\mathbf{y}, s|\mathbf{x}_0) \cdot \mathbf{n}_j = -\kappa_0 \tilde{q}_0(\mathbf{y}, s|\mathbf{x}_0) \quad |\mathbf{y}| = \rho_j. \quad (2.12c)$$

Note that the dependence of \tilde{q}_0 on \mathbf{x}_0 arises from its far-field behavior. In the case of a spherical target of radius ρ_j , we have

$$\tilde{q}_0 = G(\mathbf{x}_j, s|\mathbf{x}_0) \left(1 - \frac{\rho_j^\Lambda}{|\mathbf{y}|} \right), \quad \rho_j^\Lambda = \frac{1}{1 + \Lambda/\rho_j} \rho_j. \quad (2.13)$$

It follows that \tilde{p}_1 satisfies Eq. (2.5a) together with the singularity condition

$$\tilde{p}_1(\mathbf{x}, s|\mathbf{x}_0) \sim -\frac{1}{1 + \Lambda/\rho_j} \frac{G_{j0} \rho_j}{|\mathbf{x} - \mathbf{x}_j|} \quad \text{as } \mathbf{x} \rightarrow \mathbf{x}_j,$$

where we have set $G_{j0} = G(\mathbf{x}_j, s|\mathbf{x}_0)$. In other words, \tilde{p}_1 satisfies the inhomogeneous equation

$$D \nabla^2 \tilde{p}_1 - s \tilde{p}_1 = 4\pi D \sum_{j=1}^N G_{j0} \rho_j^\Lambda \delta(\mathbf{x} - \mathbf{x}_j), \quad \mathbf{x} \in \Omega, \quad (2.14a)$$

$$\nabla \tilde{p}_1 \cdot \mathbf{n} = 0, \quad \mathbf{x} \in \partial\Omega. \quad (2.14b)$$

This can be solved in terms of the modified Helmholtz Green's function:

$$\tilde{p}_1(\mathbf{x}, s|\mathbf{x}_0) = -4\pi D \sum_{j=1}^N G_{j0} \rho_j^\Lambda G(\mathbf{x}, s|\mathbf{x}_j). \quad (2.15)$$

We now match the far-field behavior of \tilde{q}_1 with the $O(\epsilon)$ term in the expansion of \tilde{p}_0 , see Eq. (2.11), together with the non-singular near-field behavior of \tilde{p}_1 around the j -th target. This yields

$$\tilde{q}_1(\mathbf{y}, s|\mathbf{x}_0) \rightarrow \nabla_{\mathbf{x}} G(\mathbf{x}_j, s|\mathbf{x}_0) \cdot \mathbf{y} - 4\pi D \sum_{k=1}^N G_{k0} \rho_k^\Lambda \mathcal{G}_{jk} \quad (2.16)$$

as $|\mathbf{y}| \rightarrow \infty$, where $\mathcal{G}_{ij} = G(\mathbf{x}_i, s|\mathbf{x}_j)$ for $i \neq j$, and $\mathcal{G}_{ii} = R(\mathbf{x}_i, s|\mathbf{x}_i)$. Decompose the solution around the j -th target as $\tilde{q}_1 = A_j^{(1)} + B_j^{(1)}$ with

$$A_j^{(1)} \rightarrow \chi_j^{(1)}, \quad B_j^{(1)} \rightarrow \mathbf{g}_j \cdot \mathbf{y} \text{ as } |\mathbf{y}| \rightarrow \infty,$$

with $\mathbf{g}_j = \nabla_{\mathbf{x}} G(\mathbf{x}_j, s|\mathbf{x}_0)$ and

$$\chi_j^{(1)}(\Lambda) = -4\pi D \sum_{k=1}^N G_{k0} \rho_k^\Lambda \mathcal{G}_{jk}. \quad (2.17)$$

The solution for $A_j^{(1)}$ is then

$$A_j^{(1)} = \chi_j^{(1)} \left(1 - \frac{\rho_j^\Lambda}{|\mathbf{y}|} \right). \quad (2.18)$$

In order to determine $B_j^{(1)}$, we introduce local spherical polar coordinates (r, θ, ϕ) relative to the center of the spherical target such that $\mathbf{g}_j = (0, 0, g_j)$ and $\mathbf{y} \cdot \mathbf{g}_j = g_j r \cos \theta$, $0 \leq \theta \leq \pi$. In spherical polar coordinates we have

$$\frac{\partial^2 B_j^{(1)}}{\partial r^2} + \frac{2}{r} \frac{\partial B_j^{(1)}}{\partial r} + \frac{1}{r^2 \sin \theta} \frac{\partial}{\partial \theta} \left(\sin \theta \frac{\partial B_j^{(1)}}{\partial \theta} \right) = 0, \quad r > 1, \quad (2.19a)$$

$$B_j^{(1)} \sim g_j r \cos \theta \text{ as } r \rightarrow \infty. \quad (2.19b)$$

Recall that Laplace's equation in spherical polar coordinates has the general solution

$$B(r, \theta, \phi) = \sum_{l \geq 0} \sum_{m=-l}^l \left(a_{lm} r^l + \frac{b_{lm}}{r^{l+1}} \right) P_l^m(\cos \theta) e^{im\phi}, \quad (2.20)$$

where $P_l^m(\cos \theta)$ is an associated Legendre polynomial. Imposing the Robin boundary condition and the far-field condition implies that

$$B_j^{(1)} = B_j^{(1)}(\mathbf{y}, \Lambda) = g_j \rho_j \cos \theta \left(\frac{|\mathbf{y}|}{\rho_j} + \frac{\Lambda - \rho_j}{2\Lambda + \rho_j} \frac{\rho_j^2}{|\mathbf{y}|^2} \right). \quad (2.21)$$

Combining our various results yields

$$\tilde{q}_1(\mathbf{x}, s|\mathbf{x}_0) = \chi_j^{(1)}(\Lambda) \left(1 - \frac{\rho_j^\Lambda}{|\mathbf{y}|} \right) + B_j^{(1)}(\mathbf{y}, \Lambda), \quad (2.22)$$

with $\chi_j^{(1)}$ dependent on the reaction length Λ through the matching procedure.

Although we will only consider terms up to $O(\epsilon)$, it can be shown that the n th order contribution to the inner solution in spherical polar coordinates has the general form

$$\tilde{q}_m(\mathbf{y}) = \chi_j^{(m)}(\Lambda) \left(1 - \frac{\rho_j^\Lambda}{r} \right) + \overline{B}_j^{(m)}(r, \Lambda) \quad (2.23)$$

+ higher spherical harmonics,

with $\overline{B}_j^{(m)}(r, \Lambda) = 0$ for $m = 0, 1$ and

$$\chi_j^{(m)} = -4\pi D \sum_{k=1}^N \chi_k^{(m-1)} \rho_k^\Lambda \mathcal{G}_{jk}, \quad m \geq 1, \quad (2.24)$$

with $\chi_j^{(0)} = G(\mathbf{x}_j, s|\mathbf{x}_0)$.

B. The flux into a target

The probability flux into the j -th target at time t is

$$J_j(\mathbf{x}_0, t) = -D \int_{\partial U_j} \nabla p(\mathbf{x}, t | \mathbf{x}_0) \cdot \mathbf{n}_j d\sigma \quad (2.25)$$

for $j = 1, \dots, N$, where $d\sigma$ is the surface measure. Having obtained an ϵ expansion of the inner solution in stretched coordinates, we can use it to determine a corresponding expansion of the Laplace-transformed flux:

$$\begin{aligned} \tilde{J}_j(\mathbf{x}_0, s) &= -D\epsilon^2 \int_{|\mathbf{y}|=\rho_j} \nabla \tilde{q} \cdot \mathbf{n}_j d\sigma_{\mathbf{y}} \\ &\sim -D\epsilon \int_{|\mathbf{y}|=\rho_j} [\nabla_{\mathbf{y}} \tilde{q}_0 + \epsilon \nabla_{\mathbf{y}} \tilde{q}_1 + \dots] \cdot \mathbf{n}_j d\sigma_{\mathbf{y}}. \end{aligned} \quad (2.26)$$

Using Eq. (2.23) and spherical polar coordinates, the asymptotic expansion of the flux is

$$\tilde{J}_j(\mathbf{x}_0, s) \sim \epsilon \tilde{J}_j^{(0)}(\mathbf{x}_0, s) + \epsilon^2 \tilde{J}_j^{(1)}(\mathbf{x}_0, s) + \dots, \quad (2.27)$$

with

$$\begin{aligned} \tilde{J}_j^{(m)} &= D\rho_j^2 \int_0^{2\pi} \int_0^\pi \frac{\partial}{\partial r} \bigg|_{r=\rho_j} \left[-\frac{\rho_j^\Lambda \chi_j^{(m)}}{r} + \overline{B}_j^{(m)}(r, \Lambda) \right] \\ &\quad \times \sin \theta d\theta d\phi \\ &= 4\pi D\rho_j^\Lambda \chi_j^{(m)} + 4\pi D\rho_j^2 \frac{d\overline{B}_j^{(m)}}{dr} \bigg|_{r=\rho_j}. \end{aligned} \quad (2.28)$$

In particular, the flux through the j -th target to $O(\epsilon^2)$ is

$$\begin{aligned} \tilde{J}_j(\mathbf{x}_0, s) &\sim 4\pi\epsilon D\rho_j^\Lambda \left(G(\mathbf{x}_j, s | \mathbf{x}_0) \right. \\ &\quad \left. - 4\pi\epsilon D \sum_{k=1}^N G(\mathbf{x}_k, s | \mathbf{x}_0) \rho_k^\Lambda \mathcal{G}_{jk}(s) \right) + O(\epsilon^3). \end{aligned} \quad (2.29)$$

This expansion will be valid provided that $s \ll 1/\epsilon$.

However, as we established in our previous analysis of the 3D narrow capture problem with totally absorbing targets, the limit $s \rightarrow 0$ in Eq. (2.29) is non-trivial due to the small- s singularity of the modified Helmholtz Green's function in a bounded domain [24]:

$$G(\mathbf{x}, s | \mathbf{x}') = \frac{1}{s|\Omega|} + \overline{G}(\mathbf{x}, \mathbf{x}') + sF(\mathbf{x}, \mathbf{x}') + O(s^2), \quad (2.30)$$

where $\overline{G}(\mathbf{x}, \mathbf{x}')$ is the Neumann Green's function for the diffusion equation:

$$D\nabla^2 \overline{G}(\mathbf{x}; \mathbf{x}') = \frac{1}{|\Omega|} - \delta(\mathbf{x} - \mathbf{x}'), \quad \mathbf{x} \in \Omega, \quad (2.31a)$$

$$\nabla \overline{G} \cdot \mathbf{n} = 0, \quad \mathbf{x} \in \partial\Omega, \quad (2.31b)$$

$$\overline{G}(\mathbf{x}, \mathbf{x}') = \frac{1}{4\pi D|\mathbf{x} - \mathbf{x}'|} + \overline{R}(\mathbf{x}, \mathbf{x}'), \quad \int_{\Omega} \overline{G}(\mathbf{x}, \mathbf{x}') d\mathbf{x} = 0, \quad (2.31c)$$

and $\overline{R}(\mathbf{x}, \mathbf{x}')$ is regular part of $\overline{G}(\mathbf{x}, \mathbf{x}')$. Substitution of Eq. (2.30) into Eq. (2.29) leads to terms involving factors of ϵ/s , which become arbitrarily large as $s \rightarrow 0$, thus leading to a breakdown of the ϵ expansion. Following along analogous lines to [24], it is possible to perform a partial resummation of the asymptotic expansion that renders the resulting series non-singular in the limit $s \rightarrow 0$. The basic idea is to introduce a new dimensionless parameter

$$\Gamma = \frac{4\pi\epsilon D\bar{\rho}^\Lambda}{s|\Omega|}, \quad \bar{\rho}^\Lambda = \frac{1}{N} \sum_{k=1}^N \rho_k^\Lambda. \quad (2.32)$$

This converts a subset of $O(\epsilon^n)$ terms in the expansion of \tilde{J}_j to $O(\epsilon^l \Gamma^{n-l})$ terms, $0 \leq l \leq n$. At each order of ϵ , we obtain an infinite power series in Γ that can be summed to remove all singularities in the limit $s \rightarrow 0$. Following similar steps to [24], we find that

$$\begin{aligned} \tilde{J}_j(\mathbf{x}_0, s) &\sim 4\pi\epsilon D\rho_j^\Lambda \overline{G}_{j0} \\ &\quad + \frac{\rho_j^\Lambda}{N\bar{\rho}^\Lambda} \frac{\Gamma}{1+\Gamma} \left[1 - 4\pi\epsilon D \sum_k \rho_k^\Lambda (\overline{G}_{k0} + \overline{G}_{jk}) \right] \\ &\quad + \frac{4\pi\epsilon D\rho_j^\Lambda}{(N\bar{\rho}^\Lambda)^2} \frac{\Gamma^2}{(1+\Gamma)^2} \sum_{i,k=1}^N \rho_i^\Lambda \overline{G}_{ik} \rho_k^\Lambda + O(\epsilon^2, s). \end{aligned} \quad (2.33)$$

We can now safely take the limit $s \rightarrow 0$ for $\epsilon > 0$ with $\Gamma \rightarrow \infty$.

The small- s behavior of G differs significantly in the case of the unbounded domain $\Omega = \mathbb{R}^3$. One now finds that

$$G(\mathbf{x}, s | \mathbf{x}_0) = \frac{e^{-\sqrt{s/D}|\mathbf{x}-\mathbf{x}_0|}}{4\pi D|\mathbf{x}-\mathbf{x}_0|}, \quad (2.34)$$

which is non-singular in the limit $s \rightarrow 0$. One application of diffusion to a target in an unbounded domain is calculating the effective Smoluchowski reaction rate in terms of the steady-state flux into the target. Suppose that there is a continuous concentration $c(\mathbf{x}, t)$ of non-interacting diffusing particles with background concentration c_0 , that is, $c(\mathbf{x}, t) \rightarrow c_0$ as $|\mathbf{x}| \rightarrow \infty$. The steady-state flux into the j th target is obtained by integrating over the initial position \mathbf{x}_0 according to

$$J_j = c_0 \lim_{s \rightarrow 0} s \int_{\mathbb{R}^3} \tilde{J}_j(\mathbf{x}_0, s) d\mathbf{x}_0, \quad (2.35)$$

with $\tilde{J}_j(\mathbf{x}_0, s)$ given by Eq. (2.29). Using the fact that

$$\int_{\mathbb{R}^3} G(\mathbf{x}, s | \mathbf{x}_0) d\mathbf{x}_0 = \frac{1}{s},$$

it follows that to leading order

$$J_j \approx 4\pi c_0 \epsilon D \rho_j^\Lambda = \frac{4\pi c_0 D r_j}{1 + \epsilon D / \kappa_0 r_j} \quad (2.36)$$

where $r_j = \epsilon \rho_j$ is the target radius. This recovers the modified Smoluchowski reaction rate obtained by Collins and Kimball for a partially reactive spherical surface with reactivity κ_0/ϵ [29]. In particular, note that one way to interpret the effect of imperfect reactivity is that the effective target size is reduced according to

$$r_j \rightarrow \frac{r_j}{1 + \epsilon D/\kappa_0 r_j},$$

thus making it more difficult for a diffusing molecule to encounter it. We will find that this result generalizes to other types of diffusion-mediated surface reactions, see Sect. V.

C. Splitting probabilities and first passage times

The probability that the particle is captured by the k -th target after time t is

$$\Pi_k(\mathbf{x}_0, t) = \int_t^\infty J_k(\mathbf{x}_0, t') dt', \quad (2.37)$$

and the corresponding splitting probability is

$$\pi_k(\mathbf{x}_0) = \Pi_k(\mathbf{x}_0, 0) = \int_0^\infty J_k(\mathbf{x}_0, t') dt' = \tilde{J}_k(\mathbf{x}_0, 0). \quad (2.38)$$

Introduce the survival probability that the particle hasn't been absorbed by a target in the time interval $[0, t]$, having started at \mathbf{x}_0 :

$$S(\mathbf{x}_0, t) = \int_{\Omega \setminus \mathcal{U}_a} p(\mathbf{x}, t | \mathbf{x}_0) d\mathbf{x}. \quad (2.39)$$

Differentiating both sides of this equation with respect to t and using Eqs. (2.1) implies that

$$\begin{aligned} \frac{\partial S(\mathbf{x}_0, t)}{\partial t} &= D \int_{\Omega \setminus \mathcal{U}_a} \nabla \cdot \nabla p(\mathbf{x}, t | \mathbf{x}_0) d\mathbf{x} \\ &= D \sum_{k=1}^N \int_{\partial \mathcal{U}_k} \nabla p(\mathbf{x}, t | \mathbf{x}_0) \cdot \mathbf{n} d\sigma \\ &= - \sum_{k=1}^N J_k(\mathbf{x}_0, t). \end{aligned} \quad (2.40)$$

Laplace transforming Eq. (2.40) and noting that $S(\mathbf{x}_0, 0) = 1$ gives

$$s \tilde{S}(\mathbf{x}_0, s) - 1 = - \sum_{k=1}^N \tilde{J}_k(\mathbf{x}_0, s). \quad (2.41)$$

Taking the limit $s \rightarrow 0$ then implies that $\sum_{k=1}^N \pi_k(\mathbf{x}_0) = 1$. In other words, in the case of reflecting exterior boundary $\partial\Omega$, the diffusing particle eventually finds a target with probability one.

Since the probability of the particle being captured by the k -th target is typically less than unity ($\pi_k < 1$), it

follows that the moments of the corresponding FPT density are infinite unless we condition on the given event. The FPT \mathcal{T}_k to be captured by the k -th target is

$$\mathcal{T}_k(\mathbf{x}_0) = \inf\{t > 0; \mathbf{X}(t) \in \partial \mathcal{U}_k | \mathbf{X}(0) = \mathbf{x}_0\}, \quad (2.42)$$

with $\mathcal{T}_k = \infty$ if the particle is captured by another target. Introducing the set of events $\Omega_k = \{\mathcal{T}_k < \infty\}$, we can then define the conditional FPT density according to

$$\begin{aligned} f_k(\mathbf{x}_0, t) dt &= \mathbb{P}[t < \mathcal{T}_k < t + dt | \mathcal{T}_k < \infty, \mathbf{X}(0) = \mathbf{x}_0] \\ &= \mathbb{P}[t < \mathcal{T}_k < t + dt | \mathbf{X}(0) = \mathbf{x}_0] / \mathbb{P}[\Omega_k] \\ &= \frac{\Pi_k(\mathbf{x}_0, t) - \Pi_k(\mathbf{x}_0, t + dt)}{\pi_k(\mathbf{x}_0)} \\ &= - \frac{1}{\pi_k(\mathbf{x}_0)} \frac{\partial \Pi_k(\mathbf{x}_0, t)}{\partial t} dt, \end{aligned}$$

since $\pi_k = \mathbb{P}[\Omega_k]$. That is,

$$f_k(\mathbf{x}_0, t) = \frac{J_k(\mathbf{x}_0, t)}{\pi_k(\mathbf{x}_0)}. \quad (2.43)$$

Hence, the Laplace transform of $f_k(\mathbf{x}_0, t)$ is the generator of the moments of the conditional FPT density:

$$\mathbb{E}[e^{-s\mathcal{T}_k} | \Omega_k] = \tilde{f}_k(\mathbf{x}_0, s) = \frac{\tilde{J}_k(\mathbf{x}_0, s)}{\tilde{J}_k(\mathbf{x}_0, 0)}, \quad (2.44)$$

and

$$\begin{aligned} T_k^{(n)} &= \mathbb{E}[\mathcal{T}_k^n | \Omega_k] = \left(-\frac{d}{ds} \right)^n \mathbb{E}[e^{-s\mathcal{T}_k} | \Omega_k] \Big|_{s=0} \\ &= \left(-\frac{d}{ds} \right)^n \tilde{f}_k(\mathbf{x}_0, s) \Big|_{s=0}. \end{aligned} \quad (2.45)$$

In particular, the conditional MFPT $T_k = T_k^{(1)}$ is

$$\begin{aligned} \pi_k(\mathbf{x}_0) T_k(\mathbf{x}_0) &= -\pi_k(\mathbf{x}_0) \left. \frac{d \tilde{f}_k(\mathbf{x}_0, s)}{ds} \right|_{s=0} \\ &= \tilde{\Pi}_k(\mathbf{x}_0, 0) = \lim_{s \rightarrow 0} \left. \frac{d \tilde{J}_k(\mathbf{x}_0, s)}{ds} \right|_{s=0}. \end{aligned} \quad (2.46)$$

An asymptotic expansion of the splitting probability $\pi_j(\mathbf{x}_0)$ defined in Eq. (2.38) can now be obtained by taking the limit $s \rightarrow 0$ in Eq. (2.33):

$$\begin{aligned} \pi_j(\mathbf{x}_0) &\sim \lim_{s \rightarrow 0} \tilde{J}_j(\mathbf{x}_0, s) \sim \frac{\rho_j^\Lambda}{N \bar{\rho}^\Lambda} \\ &\quad + 4\pi\epsilon D \rho_j^\Lambda \left[\bar{G}(\mathbf{x}_j, \mathbf{x}_0) - \frac{1}{N \bar{\rho}^\Lambda} \sum_{k=1}^N \rho_k^\Lambda \bar{G}(\mathbf{x}_k, \mathbf{x}_0) \right] \\ &\quad + \epsilon \bar{\eta}_j + O(\epsilon^2), \end{aligned} \quad (2.47)$$

where

$$\bar{\eta}_j = - \frac{4\pi\rho_j^\Lambda D}{N \bar{\rho}^\Lambda} \left[\sum_{k=1}^N \bar{G}_{jk} \rho_k^\Lambda - \frac{1}{N \bar{\rho}^\Lambda} \sum_{i,k=1}^N \rho_i^\Lambda \bar{G}_{ik} \rho_k^\Lambda \right]. \quad (2.48)$$

Next we consider the $O(1/\epsilon)$ and $O(1)$ terms in the asymptotic expansion of the conditional MFPT given by Eq. (2.46). For these contributions the only s -dependence is via the Γ -dependence in Eq. (2.33). Since $\Gamma = \bar{\Gamma}/s$ with $\bar{\Gamma}$ independent of s , it follows that

$$\begin{aligned} \frac{d}{ds} \frac{\Gamma^n}{(1 + \Gamma)^n} &= \frac{d}{ds} \frac{\bar{\Gamma}^n}{(s + \bar{\Gamma})^n} \\ &= -\frac{n\bar{\Gamma}^n}{(s + \bar{\Gamma})^{n+1}} \rightarrow -\frac{n}{\bar{\Gamma}} \text{ as } s \rightarrow 0. \end{aligned} \quad (2.49)$$

Hence, differentiating Eq. (2.33) with respect to s and taking $s \rightarrow 0$ gives

$$\begin{aligned} \pi_k(\mathbf{x}_0)T_k(\mathbf{x}_0) &\sim \frac{\rho_j^\Lambda |\Omega|}{4\pi D\epsilon [N\bar{\rho}^\Lambda]^2} \left[1 - 4\pi\epsilon D \sum_k \rho_k^\Lambda \bar{G}(\mathbf{x}_k, \mathbf{x}_0) \right. \\ &\quad \left. - 4\pi\epsilon D \sum_k \rho_k^\Lambda \bar{G}_{jk} \right] \\ &\quad + \frac{2\rho_j^\Lambda |\Omega|}{[N\bar{\rho}^\Lambda]^3} \sum_{i,k=1}^N \rho_i^\Lambda \bar{G}_{ik} \rho_k^\Lambda + O(\epsilon). \end{aligned} \quad (2.50)$$

In the limit $\Lambda \rightarrow 0$ (totally absorbing targets), we have $\rho_j^\Lambda \rightarrow \rho_j$ and we recover the expressions previously derived in Refs. [16, 24].

III. BOUNDARY LOCAL TIME AND THE PROPAGATOR

In this section we introduce the encounter-based formulation of diffusion-mediated surface reactions developed in Ref. [42]. We begin by giving a brief heuristic definition of the boundary local time. For more rigorous treatments see Refs. [32–34]. Consider the Brownian motion $X_t \in \mathbb{R}$, and let $\mathcal{T}(A, t)$ denote the occupation time of the set $A \subset \mathbb{R}$ during the time interval $[0, t]$:

$$\mathcal{T}(A, t) = \int_0^t I_A(X_\tau) d\tau. \quad (3.1)$$

Here $I_A(x)$ denotes the indicator function of the set $A \subset \mathbb{R}$, that is, $I_A(x) = 1$ if $x \in A$ and is zero otherwise. From the definition of the occupation time, the local time density $\mathcal{T}(a, t)$ at a point $a \in \mathbb{R}$ is defined by setting $A = [a - h, a + h]$ and taking

$$\mathcal{T}(a, t) = \lim_{\epsilon \rightarrow 0^+} \frac{1}{2h} \int_0^t I_{[a-h, a+h]}(X_s) ds. \quad (3.2)$$

We thus have the following formal representation of the local time density:

$$\mathcal{T}(a, t) = \int_0^t \delta(X_\tau - a) d\tau, \quad (3.3)$$

where $\mathcal{T}(a, t)da$ is the amount of time the Brownian particle spends in the infinitesimal interval $[a, a + da]$. Note,

in particular, that

$$\int_{-\infty}^{\infty} \mathcal{T}(a, t) da = \int_{-\infty}^{\infty} \int_0^t \delta(X_\tau - a) d\tau da = \int_0^t d\tau = t.$$

As we mentioned in the introduction, local time plays an important role in the pathwise formulation of reflected Brownian motion [33]. For the sake of illustration, consider a Wiener process confined to the interval $[0, L]$ with reflecting boundaries at $x = 0, L$. Sample paths are generated from the stochastic differential equation

$$dX(t) = \sqrt{2D}dW(t) + Dd\mathcal{T}(0, t) - Dd\mathcal{T}(L, t), \quad (3.4)$$

where $\mathcal{T}(x, t)$ is given by Eq. (3.3) so that, formally speaking,

$$d\mathcal{T}(0, t) = \delta(X_t) dt, \quad d\mathcal{T}(L, t) = \delta(X_t - L) dt.$$

In other words, each time the Brownian particle hits the end at $x = 0$ ($x = L$) it is given an impulsive kick to the right (left). Following Ref. [42], we now define the boundary local time for diffusion in a bounded domain $\Omega \subset \mathbb{R}^d$ with a totally reflecting surface $\partial\Omega$:

$$\ell_t = \lim_{h \rightarrow 0} \frac{D}{h} \int_0^t \Theta(h - \text{dist}(\mathbf{X}_\tau, \partial\Omega)) d\tau, \quad (3.5)$$

where Θ is the Heaviside function. Note that ℓ_t has units of length due to the additional factor of D .

Given the definition of the boundary local time ℓ_t for reflected Brownian motion at a surface $\partial\Omega$, one can construct partially reflected Brownian motion by introducing the stopping time [38, 39, 42]

$$\mathcal{T}_\gamma = \inf\{t > 0 : \ell_t > \hat{\ell}\}, \quad (3.6)$$

with $\hat{\ell}$ an exponentially distributed random variable that represents a stopping local time. That is, $\mathbb{P}[\hat{\ell} > \ell] = e^{-\gamma\ell}$ with $\gamma = \Lambda^{-1} = \kappa_0/D$. Let $p(\mathbf{x}, t|\mathbf{x}_0, \gamma)$ be the probability density for a Brownian particle to be at position $\mathbf{x} \in \Omega$ at time t , having started at \mathbf{x}_0 and given a constant inverse reaction length γ . Then

$$\frac{\partial p(\mathbf{x}, t|\mathbf{x}_0, \gamma)}{\partial t} = D\nabla^2 p(\mathbf{x}, t|\mathbf{x}_0, \gamma), \quad \mathbf{x} \in \Omega \quad (3.7a)$$

$$\nabla p(\mathbf{x}, t|\mathbf{x}_0, \gamma) \cdot \mathbf{n} = -\gamma p(\mathbf{x}, t|\mathbf{x}_0, \gamma), \quad \mathbf{x} \in \partial\Omega, \quad (3.7b)$$

$$p(\mathbf{x}, 0|\mathbf{x}_0, \gamma) = \delta(\mathbf{x} - \mathbf{x}_0). \quad (3.7c)$$

More precisely, p is the probability density of a particle that hasn't yet undergone a surface reaction:

$$p(\mathbf{x}, t|\mathbf{x}_0, \gamma) d\mathbf{x} = \mathbb{P}[\mathbf{X}_t \in (\mathbf{x}, \mathbf{x} + d\mathbf{x}), t < \mathcal{T}_\gamma | \mathbf{X}_0 = \mathbf{x}_0].$$

Given that ℓ_t is a nondecreasing process, the condition $t < \mathcal{T}_\gamma$ is equivalent to the condition $\ell_t < \hat{\ell}$. This implies that [42]

$$\begin{aligned} p(\mathbf{x}, t|\mathbf{x}_0, \gamma) d\mathbf{x} &= \mathbb{P}[\mathbf{X}_t \in (\mathbf{x}, \mathbf{x} + d\mathbf{x}), \ell_t < \hat{\ell} | \mathbf{X}_0 = \mathbf{x}_0] \\ &= \int_0^{\infty} d\ell \gamma e^{-\gamma\ell} \mathbb{P}[\mathbf{X}_t \in (\mathbf{x}, \mathbf{x} + d\mathbf{x}), \ell_t < \ell | \mathbf{X}_0 = \mathbf{x}_0] \\ &= \int_0^{\infty} d\ell \gamma e^{-\gamma\ell} \int_0^\ell d\ell' [P(\mathbf{x}, \ell', t|\mathbf{x}_0) d\mathbf{x}], \end{aligned}$$

where $P(\mathbf{x}, \ell, t|\mathbf{x}_0)$ is the joint probability of the position \mathbf{X}_t and boundary local time ℓ_t of reflected Brownian motion. We shall refer to P as the propagator. (Note that Grebenkov refers to the density p as the conventional propagator and denotes it by the symbol G [42, 43]. The corresponding joint probability density P is called the full propagator. In our paper we use G to denote a Neumann Green's function and simply refer to P as the propagator of reflected Brownian motion.) Using the identity

$$\int_0^\infty d\ell f(\ell) \int_0^\ell d\ell' g(\ell') = \int_0^\infty d\ell' g(\ell') \int_{\ell'}^\infty d\ell f(\ell)$$

for arbitrary integrable functions f, g , it follows that

$$p(\mathbf{x}, t|\mathbf{x}_0, \gamma) = \int_0^\infty e^{-\gamma\ell} P(\mathbf{x}, \ell, t|\mathbf{x}_0) d\ell. \quad (3.8)$$

Since the Robin boundary condition maps to an exponential law for the stopping local time $\hat{\ell}_t$, the probability density $p(\mathbf{x}, t|\mathbf{x}_0, \gamma)$ can be expressed in terms of the Laplace transform of the propagator $P(\mathbf{x}, \ell, t|\mathbf{x}_0)$ with respect to the local time ℓ .

The crucial observation is that one is free to change the probability distribution of the stopping local time $\hat{\ell}$. Given some distribution $\Psi(\ell) = \mathbb{P}[\hat{\ell} > \ell]$, one can define a generalized partially reflecting Brownian motion whose probability density is given by [42]

$$p^\Psi(\mathbf{x}, t|\mathbf{x}_0) = \int_0^\infty \Psi(\ell) P(\mathbf{x}, \ell, t|\mathbf{x}_0) d\ell. \quad (3.9)$$

In other words, the encounter-based formulation provides a framework for exploring a range of surface reaction mechanisms that go well beyond the constant reactivity case and exponential law $\Psi(\ell) = e^{-\ell/\Lambda}$ associated with the Robin boundary condition. For example, one could consider a reactivity $\kappa(\ell)$ that depends on the local time ℓ (or the rescaled number of surface encounters). The corresponding distribution of the stopping local time $\hat{\ell}$ would then be

$$\Psi(\ell) = \exp\left(-\frac{1}{D} \int_0^\ell \kappa(\ell') d\ell'\right). \quad (3.10)$$

However, in order to calculate the probability density $p^\Psi(\mathbf{x}, t|\mathbf{x}_0)$ for a more general surface reaction mechanism, it is not usually possible to solve a corresponding BVP since the Robin boundary condition no longer holds. This motivates the construction of the propagator $P(\mathbf{x}, \ell, t|\mathbf{x}_0)$, which is carried out in Ref. [42] using a non-standard integral representation of the probability density $p(\mathbf{x}, t|\mathbf{x}_0, \gamma)$ and spectral properties of the so-called Dirichlet-to-Neumann operator. In this paper it will be more convenient to work directly with the BVP for the propagator. In the case of a bounded domain Ω with partially reactive boundary $\partial\Omega$, the BVP takes the

following form [42]:

$$\frac{\partial P(\mathbf{x}, \ell, t|\mathbf{x}_0)}{\partial t} = D\nabla^2 P(\mathbf{x}, \ell, t|\mathbf{x}_0), \quad \mathbf{x} \in \Omega \quad (3.11a)$$

$$- D\nabla P(\mathbf{x}, \ell, t|\mathbf{x}_0) \cdot \mathbf{n} = -D\nabla p_\infty(\mathbf{x}, t|\mathbf{x}_0) \cdot \mathbf{n} \delta(\ell) \\ + D \frac{\partial}{\partial \ell} P(\mathbf{x}, \ell, t|\mathbf{x}_0), \quad \mathbf{x} \in \partial\Omega, \quad (3.11b)$$

$$P(\mathbf{x}, \ell = 0, t|\mathbf{x}_0) = -\nabla p_\infty(\mathbf{x}, t|\mathbf{x}_0) \cdot \mathbf{n}, \quad \mathbf{x} \in \partial\Omega \quad (3.11c)$$

$$\lim_{\ell \rightarrow \infty} P(\mathbf{x}, \ell, t|\mathbf{x}_0) = 0, \quad (3.11d)$$

$$P(\mathbf{x}, \ell, 0|\mathbf{x}_0) = \delta(\mathbf{x} - \mathbf{x}_0)\delta(\ell), \quad \mathbf{x} \in \Omega, \quad (3.11e)$$

where p_∞ is the probability density for a totally absorbing surface,

$$p_\infty(\mathbf{x}, t|\mathbf{x}_0) = \lim_{\gamma \rightarrow \infty} p(\mathbf{x}, t|\mathbf{x}_0, \gamma). \quad (3.12)$$

Note that multiplying the boundary condition (3.11b) by $e^{-\gamma\ell}$, integrating with respect to $\ell \in [0, \infty)$, and using integration by parts combined with Eq. (3.11c) recovers the standard Robin boundary condition for $p(\mathbf{x}, t|\mathbf{x}_0, \gamma)$. In appendix A we present an alternative derivation of Eq. (3.11) that is based on a Feynman-Kac equation, see also Ref. [44].

IV. NARROW CAPTURE PROBLEM: GENERALIZED SURFACE REACTIONS

In this section we use the encounter-based formulation [42] to analyze the narrow capture problem shown in Fig. 1 in the case of more general diffusion-mediated surface reactions. For simplicity, we take each target to have the same rule for surface reactions so that we only need to keep track of a single boundary local time that does not distinguish between targets. The BVP for the propagator of the system shown in Fig. 1 can then be written down by analogy with Eq. (3.11). Again it will be more convenient to work in Laplace space so that

$$D\nabla^2 \tilde{P}(\mathbf{x}, \ell, s|\mathbf{x}_0) - s\tilde{P}(\mathbf{x}, \ell, s|\mathbf{x}_0) \\ = -\delta(\mathbf{x} - \mathbf{x}_0)\delta(\ell), \quad \mathbf{x} \in \Omega \setminus \mathcal{U}_a, \quad (4.1a)$$

$$\nabla \tilde{P}(\mathbf{x}, \ell, s|\mathbf{x}_0) \cdot \mathbf{n} = 0, \quad \mathbf{x} \in \partial\Omega, \quad (4.1b)$$

$$- D\nabla \tilde{P}(\mathbf{x}, \ell, s|\mathbf{x}_0) \cdot \mathbf{n}_k = -D\nabla \tilde{p}_\infty(\mathbf{x}, s|\mathbf{x}_0) \cdot \mathbf{n}_k \delta(\ell) \\ + D \frac{\partial}{\partial \ell} \tilde{P}(\mathbf{x}, \ell, s|\mathbf{x}_0), \quad \mathbf{x} \in \partial\mathcal{U}_k, \quad (4.1c)$$

$$\tilde{P}(\mathbf{x}, \ell, s|\mathbf{x}_0) \Big|_{\ell=0} = -\nabla \tilde{p}_\infty(\mathbf{x}, s|\mathbf{x}_0) \cdot \mathbf{n}_k, \quad \mathbf{x} \in \partial\mathcal{U}_k, \quad (4.1d)$$

$$\lim_{\ell \rightarrow \infty} \tilde{P}(\mathbf{x}, \ell, s|\mathbf{x}_0) = 0, \quad \mathbf{x} \in \Omega \setminus \mathcal{U}_a. \quad (4.1e)$$

A. Asymptotic expansion of the propagator

Following along analogous lines to the asymptotic analysis of Sect. II, we separately consider outer and inner solutions for the propagator. In the outer region,

$\tilde{P}(\mathbf{x}, \ell, s | \mathbf{x}_0)$ is expanded as

$$\begin{aligned}\tilde{P}(\mathbf{x}, \ell, s | \mathbf{x}_0) &\sim G(\mathbf{x}, s | \mathbf{x}_0) \delta(\ell) + \epsilon \tilde{P}_1(\mathbf{x}, \ell, s | \mathbf{x}_0) \\ &\quad + \epsilon^2 \tilde{P}_2(\mathbf{x}, \ell, s | \mathbf{x}_0) + \dots,\end{aligned}$$

where G is the Neumann Green's function of the modified Helmholtz equation as defined in Eq. (2.4), and (for $m \geq 1$)

$$\begin{aligned}D\nabla^2 \tilde{P}_m(\mathbf{x}, \ell, s | \mathbf{x}_0) - s \tilde{P}_m(\mathbf{x}, \ell, s | \mathbf{x}_0) &= 0, \\ \mathbf{x} \in \Omega \setminus \{\mathbf{x}_1, \dots, \mathbf{x}_N\},\end{aligned}\tag{4.2a}$$

$$\nabla \tilde{P}_m(\mathbf{x}, \ell, s | \mathbf{x}_0) \cdot \mathbf{n} = 0, \quad \mathbf{x} \in \partial\Omega,\tag{4.2b}$$

$$\lim_{\ell \rightarrow \infty} \tilde{P}_m(\mathbf{x}, \ell, s | \mathbf{x}_0) = 0, \quad \mathbf{x} \in \Omega \setminus \{\mathbf{x}_1, \dots, \mathbf{x}_N\}.\tag{4.2c}$$

Eqs. (4.2) are supplemented by singularity conditions as $\mathbf{x} \rightarrow \mathbf{x}_j$, $j = 1, \dots, N$, which are determined by matching to the inner solution.

Turning to the inner solution, we now need to rescale both $\mathbf{x} - \mathbf{x}_j$ and ℓ around the j th target. Therefore, we introduce the stretched coordinates $\mathbf{y} = \epsilon^{-1}(\mathbf{x} - \mathbf{x}_j)$ and $\hat{\ell} = \ell/\epsilon$, and take $\tilde{Q}(\mathbf{y}, \hat{\ell}, s | \mathbf{x}_0) = \epsilon \tilde{P}(\mathbf{x}, \ell, s | \mathbf{x}_0)$ to be the corresponding inner solution. Eq. (4.1) then implies that

$$D\nabla_{\mathbf{y}}^2 \tilde{Q}(\mathbf{y}, \hat{\ell}, s | \mathbf{x}_0) - s\epsilon^2 \tilde{Q}(\mathbf{y}, \hat{\ell}, s | \mathbf{x}_0) = 0, \quad |\mathbf{y}| > \rho_j,\tag{4.3a}$$

$$\begin{aligned}D\nabla_{\mathbf{y}} \tilde{Q}(\mathbf{y}, \hat{\ell}, s | \mathbf{x}_0) \cdot \mathbf{n}_j &= D\nabla_{\mathbf{y}} \tilde{q}(\mathbf{y}, s | \mathbf{x}_0) \cdot \mathbf{n}_j \delta(\hat{\ell}) \\ &\quad - D \frac{\partial}{\partial \hat{\ell}} \tilde{Q}(\mathbf{y}, \hat{\ell}, s | \mathbf{x}_0), \quad |\mathbf{y}| = \rho_j,\end{aligned}\tag{4.3b}$$

$$\tilde{Q}(\mathbf{y}, \hat{\ell} = 0, s | \mathbf{x}_0) = -\nabla_{\mathbf{y}} \tilde{q}(\mathbf{y}, s | \mathbf{x}_0) \cdot \mathbf{n}_j, \quad |\mathbf{y}| = \rho_j.\tag{4.3c}$$

with $\tilde{q}(\mathbf{y}, s | \mathbf{x}_0)$ the inner solution of $p_{\infty}(\mathbf{x}, s | \mathbf{x}_0)$. The choice of scaling is consistent with a reactivity of $O(1/\epsilon)$, as assumed in Sect. II. Introducing a perturbation expansion of the inner solution around the j -th target of the form

$$\tilde{Q} \sim \tilde{Q}_0 + \epsilon \tilde{Q}_1 + \epsilon^2 \tilde{Q}_2 + O(\epsilon^3)\tag{4.4}$$

then yields the following pair of equations for $m = 0, 1$ (assuming $s \ll 1/\epsilon$):

$$D\nabla_{\mathbf{y}}^2 \tilde{Q}_m(\mathbf{y}, \hat{\ell}, s | \mathbf{x}_0) = 0, \quad |\mathbf{y}| > \rho_j,\tag{4.5a}$$

$$\begin{aligned}D\nabla_{\mathbf{y}} \tilde{Q}_m(\mathbf{y}, \hat{\ell}, s | \mathbf{x}_0) \cdot \mathbf{n}_j &= D\nabla_{\mathbf{y}} \tilde{q}_m(\mathbf{y}, s | \mathbf{x}_0) \cdot \mathbf{n}_j \delta(\hat{\ell}) \\ &\quad - D \frac{\partial}{\partial \hat{\ell}} \tilde{Q}_m(\mathbf{y}, \hat{\ell}, s | \mathbf{x}_0), \quad |\mathbf{y}| = \rho_j,\end{aligned}\tag{4.5b}$$

$$\tilde{Q}_m(\mathbf{y}, \hat{\ell} = 0, s | \mathbf{x}_0) = -\nabla_{\mathbf{y}} \tilde{q}_m(\mathbf{y}, s | \mathbf{x}_0) \cdot \mathbf{n}_j, \quad |\mathbf{y}| = \rho_j.\tag{4.5c}$$

Here \tilde{q}_m is the m th term in the asymptotic expansion of the inner solution of the probability density in the case of totally absorbing targets. For $m = 0, 1$ it is obtained by taking the limit $\Lambda \rightarrow 0$ in Eqs. (2.13) and (2.22), respectively. Eqs. (4.5) are supplemented by far-field conditions obtained by matching with the non-singular

near-field behavior of the outer solution. In order to perform the matching, it is again necessary to take into account the Taylor expansion of G near the j -th target, see Eq. (2.11).

Let us begin with the leading order contribution to the inner solution. Matching the far-field behavior of \tilde{Q}_0 with the near-field behavior of $\epsilon \tilde{P}_0$ shows that the general solution to Eq. (4.5a) for $m = 0$ is of the form

$$\tilde{Q}_0(\mathbf{y}, \hat{\ell}, s | \mathbf{x}_0) = G(\mathbf{x}_j, s | \mathbf{x}_0) \left(1 - \frac{\rho_j}{|\mathbf{y}|}\right) \delta(\hat{\ell}) + \frac{c_j(\hat{\ell})}{|\mathbf{y}|}.\tag{4.6}$$

Note that the function multiplying $\delta(\hat{\ell})$ is \tilde{q}_0 so that substituting (4.6) into the boundary conditions (4.5b,c) implies that

$$\frac{dc_j(\hat{\ell})}{d\hat{\ell}} + \rho_j^{-1} c_j(\hat{\ell}) = 0, \quad c_j(0) = G(\mathbf{x}_j, s | \mathbf{x}_0).\tag{4.7}$$

Hence,

$$c_j(\hat{\ell}) = G(\mathbf{x}_j, s | \mathbf{x}_0) e^{-\hat{\ell}/\rho_j}\tag{4.8}$$

and

$$\tilde{Q}_0(\mathbf{y}, \hat{\ell}, s | \mathbf{x}_0) = G(\mathbf{x}_j, s | \mathbf{x}_0) \left[\left(1 - \frac{\rho_j}{|\mathbf{y}|}\right) \delta(\hat{\ell}) + \frac{e^{-\hat{\ell}/\rho_j}}{|\mathbf{y}|} \right].\tag{4.9}$$

Rewriting Eq. (4.9) in terms of the original unstretched coordinates then determines the singularity condition for \tilde{P}_1 :

$$\tilde{P}_1(\mathbf{x}, \ell, s | \mathbf{x}_0) \sim -\frac{G_{j0}}{|\mathbf{x} - \mathbf{x}_j|} \left[\rho_j \delta(\ell) - e^{-\ell/\epsilon\rho_j} \right] \quad \text{as } \mathbf{x} \rightarrow \mathbf{x}_j,$$

where $G_{j0} = G(\mathbf{x}_j, s | \mathbf{x}_0)$. The solution of Eq. (4.2) for $m = 1$ is thus given by

$$\begin{aligned}\tilde{P}_1(\mathbf{x}, \ell, s | \mathbf{x}_0) &= -4\pi D \sum_{j=1}^N G_{j0} \left[\rho_j \delta(\ell) - e^{-\ell/\epsilon\rho_j} \right] G(\mathbf{x}, s | \mathbf{x}_j).\end{aligned}\tag{4.10}$$

We now match the far-field behavior of \tilde{Q}_1 with the $O(\epsilon)$ term in the expansion of $G(\mathbf{x}, s | \mathbf{x}_0)$ about \mathbf{x}_j (multiplied by $\delta(\ell)$) together with the non-singular near-field behavior of \tilde{P}_1 around the j -th target. This yields

$$\begin{aligned}\tilde{Q}_1(\mathbf{y}, \hat{\ell}, s | \mathbf{x}_0) &\rightarrow \nabla_{\mathbf{x}} G(\mathbf{x}_j, s | \mathbf{x}_0) \cdot \mathbf{y} \delta(\hat{\ell}) \\ &\quad - 4\pi D \sum_{k=1}^N G_{k0} \left[\rho_k \delta(\hat{\ell}) - e^{-\hat{\ell}/\rho_k} \right] \mathcal{G}_{jk}\end{aligned}\tag{4.11}$$

as $|\mathbf{y}| \rightarrow \infty$, where $\mathcal{G}_{ij} = G(\mathbf{x}_i, s | \mathbf{x}_j)$ for $i \neq j$, and $\mathcal{G}_{ii} = R(\mathbf{x}_i, s | \mathbf{x}_i)$. Following the analysis of Sect. II, decompose

the solution around the j -th target as $\tilde{Q}_1 = A_j^{(1)} + B_j^{(1)}$ with

$$A_j^{(1)} \rightarrow \chi_j^{(1)}(\hat{\ell}), \quad B_j^{(1)} \rightarrow \mathbf{g}_j \cdot \mathbf{y} \delta(\hat{\ell}) \text{ as } |\mathbf{y}| \rightarrow \infty,$$

with $\mathbf{g}_j = \nabla_{\mathbf{x}} G(\mathbf{x}_j, s|\mathbf{x}_0)$ and

$$\begin{aligned} \chi_j^{(1)}(\hat{\ell}) &= -4\pi D \sum_{k=1}^N G_{k0} \left[\rho_k \delta(\hat{\ell}) - e^{-\hat{\ell}/\rho_k} \right] \mathcal{G}_{jk} \\ &= \bar{\chi}_j \delta(\hat{\ell}) + 4\pi D \sum_{k=1}^N G_{k0} e^{-\hat{\ell}/\rho_k} \mathcal{G}_{jk}, \end{aligned} \quad (4.12)$$

where

$$\bar{\chi}_j = -4\pi D \sum_{k=1}^N G_{k0} \rho_k \mathcal{G}_{jk}.$$

The general solutions for $A_j^{(1)}$ is

$$\begin{aligned} A_j^{(1)} &= \chi_j^{(1)}(\hat{\ell}) \left(1 - \frac{\rho_j}{|\mathbf{y}|} \right) + \frac{a_j(\hat{\ell})}{|\mathbf{y}|} \\ &= \bar{\chi}_j \left(1 - \frac{\rho_j}{|\mathbf{y}|} \right) \delta(\hat{\ell}) \\ &\quad + 4\pi D \left[\sum_{k=1}^N G_{k0} e^{-\hat{\ell}/\rho_k} \mathcal{G}_{jk} \right] \left(1 - \frac{\rho_j}{|\mathbf{y}|} \right) + \frac{a_j(\hat{\ell})}{|\mathbf{y}|}. \end{aligned} \quad (4.13)$$

The function multiplying $\delta(\hat{\ell})$ can be identified with the zeroth-order spherical harmonic contribution from

$\tilde{q}_1(\mathbf{y}, s|\mathbf{x}_0)$. Substituting (4.13) and (4.16) into the boundary conditions (4.5b,c) implies that

$$\frac{da_j(\hat{\ell})}{d\hat{\ell}} + \rho_j^{-1} a_j(\hat{\ell}) = 4\pi D \sum_{k=1}^N G_{k0} e^{-\hat{\ell}/\rho_k} \mathcal{G}_{jk}, \quad (4.14)$$

with $a_j(0) = \bar{\chi}_j$. Hence

$$a_j(\hat{\ell}) = \bar{\chi}_j e^{-\hat{\ell}/\rho_j} + 4\pi D \sum_{k=1}^N G_{k0} \frac{e^{-\hat{\ell}/\rho_k} - e^{-\hat{\ell}/\rho_j}}{\rho_j^{-1} - \rho_k^{-1}} \mathcal{G}_{jk}. \quad (4.15)$$

The general solution for $B_j^{(1)}$ is

$$B_j^{(1)} = g_j \rho_j \cos \theta \left(\frac{|\mathbf{y}|}{\rho_j} - \frac{\rho_j^2}{|\mathbf{y}|^2} \right) \delta(\hat{\ell}) + \frac{b_j(\hat{\ell})}{|\mathbf{y}|^2}. \quad (4.16)$$

with $b_j(\hat{\ell})$ determined by the boundary conditions (4.5b,c). That is,

$$\frac{db_j(\hat{\ell})}{d\hat{\ell}} + \frac{2}{\rho_j} b_j(\hat{\ell}) = 0, \quad b_j(0) = 3g_j \rho_j^2 \cos \theta. \quad (4.17)$$

This has the solution

$$b_j(\hat{\ell}) = 3e^{-2\hat{\ell}/\rho_j} g_j \rho_j^2 \cos \theta \quad (4.18)$$

Combining our various results yields the $O(\epsilon)$ contribution to the inner solution for the propagator:

$$\begin{aligned} \tilde{Q}_1(\mathbf{y}, \hat{\ell}, s|\mathbf{x}_0) &= \chi_j^{(1)}(\hat{\ell}) \left(1 - \frac{\rho_j}{|\mathbf{y}|} \right) + \frac{4\pi D}{|\mathbf{y}|} \left[\sum_{k=1}^N G_{k0} \left\{ \frac{e^{-\hat{\ell}/\rho_k} - e^{-\hat{\ell}/\rho_j}}{\rho_j^{-1} - \rho_k^{-1}} - \rho_k e^{-\hat{\ell}/\rho_j} \right\} \mathcal{G}_{jk} \right] \\ &\quad + g_j \rho_j \cos \theta \left[\left(\frac{|\mathbf{y}|}{\rho_j} - \frac{\rho_j^2}{|\mathbf{y}|^2} \right) \delta(\hat{\ell}) + \frac{3\rho_j e^{-2\hat{\ell}/\rho_j}}{|\mathbf{y}|^2} \right]. \end{aligned} \quad (4.19)$$

B. The generalized target flux

Having obtained an asymptotic expansion of the inner solution of the propagator in Laplace space, we can use the transform (3.9) to construct the corresponding asymptotic expansion of the probability density and then use this to determine the Laplace transformed flux into each target. First, Laplace transforming Eq. (3.9) gives

$$\tilde{p}^{\Psi}(\mathbf{x}, s|\mathbf{x}_0) = \int_0^{\infty} \Psi(\ell) \tilde{P}(\mathbf{x}, \ell, s|\mathbf{x}_0) d\ell, \quad (4.20)$$

where the superscript Ψ indicates that we are considering a generalized diffusion-mediated surface reaction. The case of Robin boundary conditions is recovered by setting

$\Psi(\ell) = e^{-q\ell}$ with $q = \kappa_0/D$ and κ_0 a constant reactivity. Recall that in the analysis of Sect. II we rescaled κ_0 according to $\kappa_0 \rightarrow \kappa_0/\epsilon$ so that $\Psi(\ell) = e^{-\kappa_0 \ell/\epsilon D} = e^{-q\hat{\ell}}$ with $\hat{\ell} = \ell/\epsilon$. Therefore, we take $\Psi = \Psi(\hat{\ell})$ and rewrite Eq. (4.20) as

$$\tilde{p}^{\Psi}(\mathbf{x}, s|\mathbf{x}_0) = \epsilon \int_0^{\infty} \Psi(\hat{\ell}) \tilde{P}(\mathbf{x}, \epsilon \hat{\ell}, s|\mathbf{x}_0) d\hat{\ell}. \quad (4.21)$$

Introducing stretched coordinates along the lines of Sect. IVA and using $\tilde{Q}(\mathbf{y}, \hat{\ell}, s|\mathbf{x}_0) = \epsilon \tilde{P}(\mathbf{x}, \ell, s|\mathbf{x}_0)$ then gives the corresponding transform of the inner solution around each target:

$$\tilde{q}^{\Psi}(\mathbf{y}, s|\mathbf{x}_0) = \int_0^{\infty} \Psi(\hat{\ell}) \tilde{Q}(\mathbf{y}, \hat{\ell}, s|\mathbf{x}_0) d\hat{\ell}. \quad (4.22)$$

Substituting the asymptotic expansion of the propagator, Eq. (4.4) and using the fact that the integral of an asymptotic expansion is also an asymptotic expansion, we have

$$\tilde{q}^\Psi \sim \tilde{q}_0^\Psi + \epsilon \tilde{q}_1^\Psi + \epsilon^2 \tilde{q}_2^\Psi + O(\epsilon^3), \quad (4.23)$$

with

$$\tilde{q}_m(\mathbf{y}, s | \mathbf{x}_0, q) = \int_0^\infty \Psi(\hat{\ell}) \tilde{Q}_m(\mathbf{y}, \hat{\ell}, s | \mathbf{x}_0) d\hat{\ell}, \quad m \geq 0. \quad (4.24)$$

Substituting Eqs. (4.9) and (4.19) into (4.24) for $m = 0$ and $m = 1$, respectively, yields

$$\tilde{q}_0^\Psi(\mathbf{y}, s | \mathbf{x}_0) = G(\mathbf{x}_j, s | \mathbf{x}_0) \left[1 - \frac{\rho_j}{|\mathbf{y}|} + \frac{\tilde{\Psi}(1/\rho_j)}{|\mathbf{y}|} \right], \quad (4.25)$$

and

$$\begin{aligned} \tilde{q}_1^\Psi(\mathbf{y}, s | \mathbf{x}_0) &= \chi_j^\Psi \left(1 - \frac{\rho_j}{|\mathbf{y}|} \right) + \frac{4\pi D}{|\mathbf{y}|} \left[\sum_{k=1}^N G_{k0} \left\{ \frac{\tilde{\Psi}(1/\rho_k) - \tilde{\Psi}(1/\rho_j)}{\rho_j^{-1} - \rho_k^{-1}} - \rho_k \tilde{\Psi}(1/\rho_j) \right\} \mathcal{G}_{jk} \right] \\ &+ g_j \rho_j \cos \theta \left[\frac{|\mathbf{y}|}{\rho_j} - \frac{\rho_j^2}{|\mathbf{y}|^2} + \frac{3\rho_j \tilde{\Psi}(2/\rho_j)}{|\mathbf{y}|^2} \right], \end{aligned} \quad (4.26)$$

with

$$\chi_j^\Psi = -4\pi D \sum_{k=1}^N G_{k0} \mathcal{F}(\rho_k) \mathcal{G}_{jk}, \quad \mathcal{F}(\rho_k) \equiv \rho_k - \tilde{\Psi}(1/\rho_k). \quad (4.27)$$

We have assumed that the Laplace transform of $\Psi(\ell)$ exists and have used the identity $\Psi(0) = 1$. It can be checked that (4.25) and (4.26) reduce to Eqs. (2.13) and (2.22), respectively, on setting $\Psi(\ell) = e^{-\gamma\ell}$ and $\tilde{\Psi}(q) = (q + \gamma)^{-1}$, see appendix B.

Given an asymptotic expansion of the inner solution $\tilde{q}^\Psi(\mathbf{y}, s | \mathbf{x}_0)$, we can determine the Laplace transformed flux into each target along analogous lines to the derivation of Eq. (2.29). In the case of the j -th target, we have

$$\tilde{J}_j^\Psi(\mathbf{x}_0, s) \sim \epsilon \tilde{J}_{j,0}^\Psi(\mathbf{x}_0, s) + \epsilon^2 \tilde{J}_{j,1}^\Psi(\mathbf{x}_0, s) + \dots, \quad (4.28)$$

with (in spherical polar coordinates)

$$\tilde{J}_{j,m}^\Psi = D \rho_j^2 \int_0^{2\pi} \int_0^\pi \frac{\partial \tilde{q}_m(\mathbf{y}, s | \mathbf{x}_0)}{\partial r} \Big|_{r=\rho_j} \sin \theta d\theta d\phi. \quad (4.29)$$

It then follows from Eqs. (4.25) and (4.26) that

$$\begin{aligned} \tilde{J}_j(\mathbf{x}_0, s) &\sim 4\pi \epsilon D \left[\mathcal{F}(\rho_j) G(\mathbf{x}_j, s | \mathbf{x}_0) \right. \\ &\quad \left. - 4\pi \epsilon D \sum_{k=1}^N G(\mathbf{x}_k, s | \mathbf{x}_0) \left\{ \frac{\rho_k^2 \mathcal{F}(\rho_j) - \rho_j^2 \mathcal{F}(\rho_k)}{\rho_k - \rho_j} \right\} \mathcal{G}_{jk}(s) \right] \\ &\quad + O(\epsilon^3). \end{aligned} \quad (4.30)$$

It can be checked that $\mathcal{F}(\rho_j) \rightarrow \rho_j^\Lambda$ and

$$\frac{\rho_k^2 \mathcal{F}(\rho_j) - \rho_j^2 \mathcal{F}(\rho_k)}{\rho_k - \rho_j} \rightarrow \rho_j^\Lambda \rho_k^\Lambda$$

on setting $\Psi(\ell) = e^{-\ell/\Lambda}$ and Eq. (4.30) reduces to Eq. (2.29).

V. EFFECTIVE TARGET RADIUS FOR GENERALIZED SURFACE REACTIONS

There are many different quantities that we could consider in order to illustrate the above theory. Here we will restrict ourselves to the leading order terms in the splitting probabilities and conditional MFPTs. Using similar arguments to Sect. IIIC, one finds that

$$\pi_k(\mathbf{x}_0) \sim \frac{\rho_j - \tilde{\Psi}(1/\rho_j)}{\sum_{k=1}^N (\rho_k - \tilde{\Psi}(1/\rho_k))} + O(\epsilon), \quad (5.1)$$

$$\pi_k(\mathbf{x}_0) T_k(\mathbf{x}_0) \sim \frac{(\rho_j - \tilde{\Psi}(1/\rho_j)) |\Omega|}{4\pi D \epsilon \left[\sum_{k=1}^N (\rho_k - \tilde{\Psi}(1/\rho_k)) \right]^2} + O(1). \quad (5.2)$$

It can be seen that these expressions are independent of the Neumann Green's function G and, hence, of any details regarding the bulk domain Ω . and the positions \mathbf{x}_j of the targets. On the other hand, they strongly depend on the surface reactions via the renormalized target radii $\mathcal{F}(\rho_k)$, $k = 1, \dots, N$. For the sake of illustration, we list

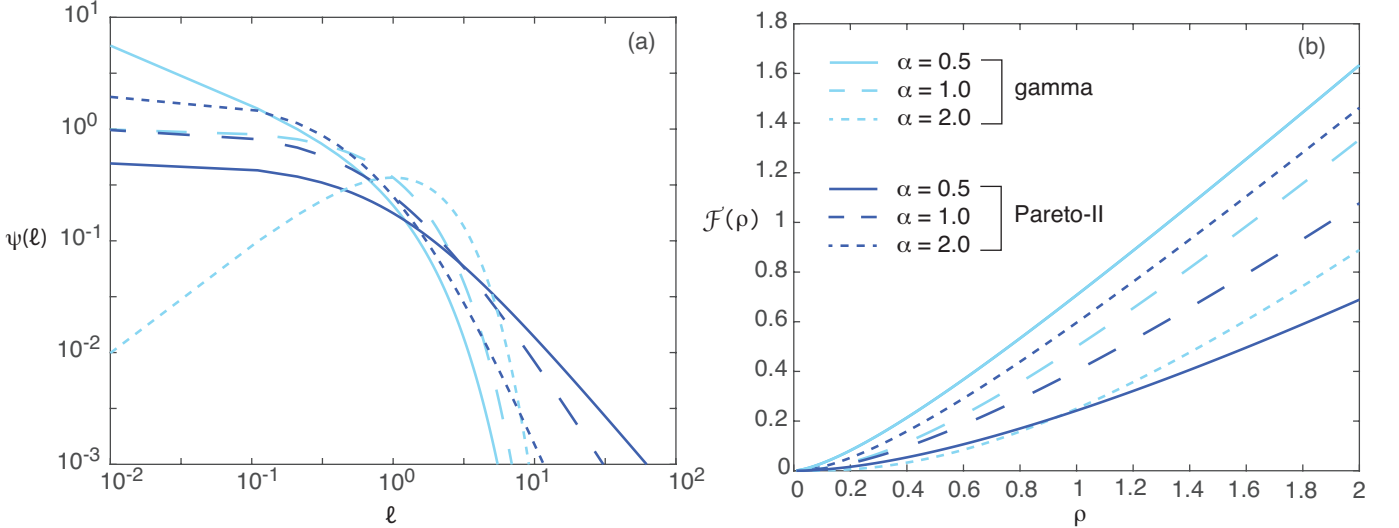


FIG. 2. (a) Plots of the probability density $\psi(\ell)$ as a function of the stopping local time for the gamma and Pareto-II models. (b) Corresponding plots of the renormalized target radius $\mathcal{F}(\rho)$ as a function of the physical radius ρ . We also set $\gamma = \kappa_0/D = 1$.

a few possible surface reaction models in terms of the probability density $\psi(\ell)$, where

$$\psi(\ell) = -\frac{d\Psi(\ell)}{d\ell}, \quad \tilde{\psi}(q) = 1 - q\tilde{\Psi}(q), \quad (5.3)$$

and the equivalent encounter-dependent reactivity $\kappa(\ell)$ defined in Eq. (3.10). See Table 1 of Ref. [42] for a more comprehensive list. In each case we take $\gamma = \kappa_0/D$ where κ_0 is some reference reactivity.

(a) *Exponential distribution.*

$$\psi(\ell) = \gamma e^{-\gamma\ell}, \quad \tilde{\psi}(q) = \frac{\gamma}{\gamma + q}, \quad \kappa(\ell) = \kappa_0. \quad (5.4)$$

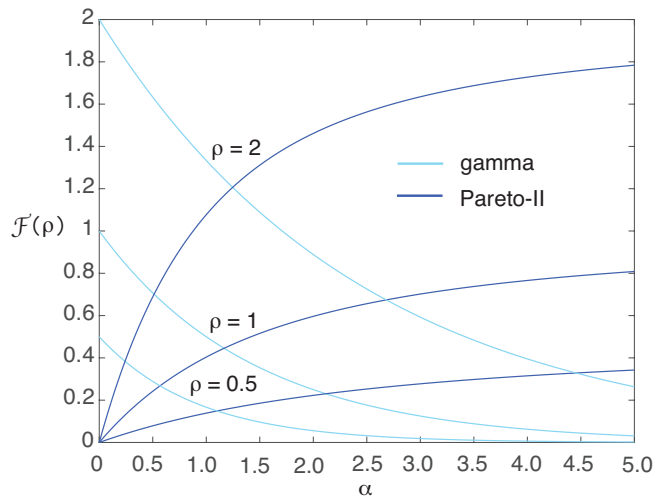


FIG. 3. Plots of $\mathcal{F}(\rho)$ for $\rho = 0.5, 1, 2$ as a function of the coefficient α for the gamma and Pareto-II models.

(b) *Gamma distribution.*

$$\psi(\ell) = \frac{\gamma(\gamma\ell)^{\alpha-1} e^{-\gamma\ell}}{\Gamma(\alpha)}, \quad \tilde{\psi}(q) = \left(\frac{\gamma}{\gamma + q}\right)^\alpha, \quad (5.5a)$$

and

$$\kappa(\ell) = \kappa_0 \frac{(\gamma\ell)^{\alpha-1} e^{-\gamma\ell}}{\Gamma(\alpha, \gamma\ell)}, \quad (5.5b)$$

where $\Gamma(\alpha)$ is the gamma function and $\Gamma(\alpha, z)$ is the upper incomplete gamma function.

(c) *Pareto-II (Lomax) distribution.*

$$\psi(\ell) = \frac{\gamma\alpha}{(1 + \gamma\ell)^{1+\alpha}}, \quad \tilde{\psi}(q) = \alpha \left(\frac{q}{\gamma}\right)^\alpha e^{q/\gamma} \Gamma(-\alpha, q/\gamma), \quad (5.6a)$$

and

$$\kappa(\ell) = \kappa_0 \frac{\alpha}{1 + \gamma\ell}. \quad (5.6b)$$

In Fig. 2(a) we plot the probability density $\psi(\ell)$ as a function of the stopping local time ℓ for the gamma and Pareto-II models and the particular coefficients $\alpha = 0.5, 1, 2$. We also set $\gamma = 1$. (The gamma density for $\alpha = 1$ gives the exponential model). In Fig. 2(b) we show the corresponding plots of the renormalized target radius function $\mathcal{F}(\rho) = \rho - \tilde{\Psi}(\rho)$. In all cases, $\mathcal{F}(\rho)$ is a nonlinear, monotonically increasing function of ρ . Moreover, $\mathcal{F}(\rho)$ is sensitive to the value of the α -coefficient that parameterizes each of the two probability distributions. That is, $\mathcal{F}(\rho)$ is a decreasing (increasing) function of α for fixed ρ in the case of the gamma (Pareto-II) model. Having determined the renormalized radius $\mathcal{F}(\rho)$, we can now explore how the choice of surface reaction model modifies the leading-order contributions to

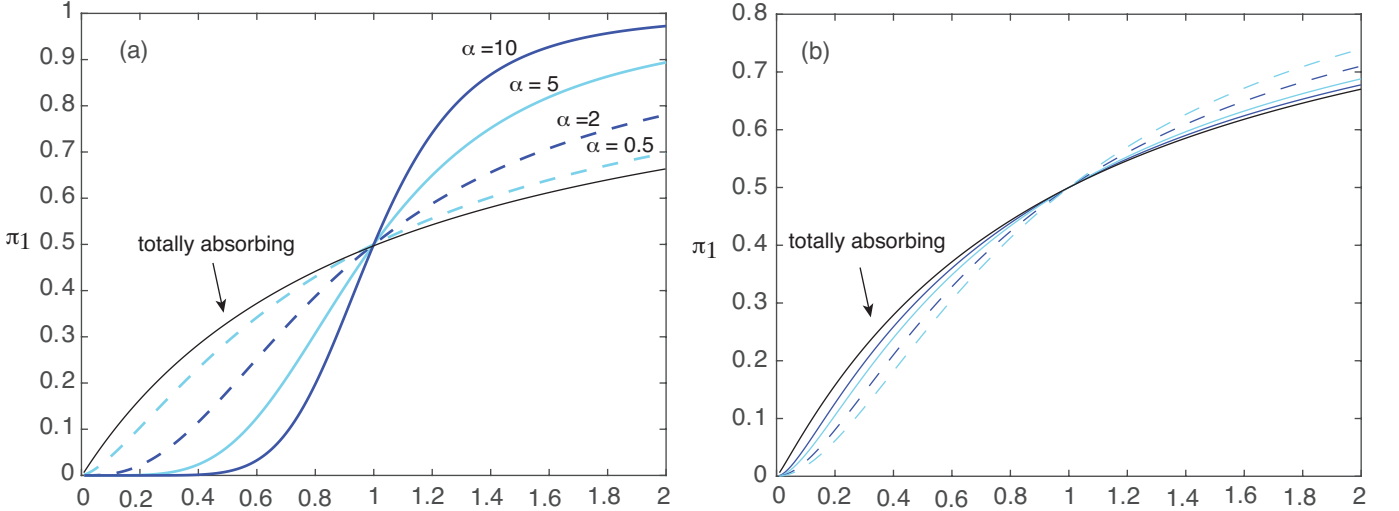


FIG. 4. Two spherical targets with rescaled radii ρ_1 and ρ_2 . Plot of leading-order contribution to the splitting probability of the first target, $\pi_1 \sim \mathcal{F}(\rho_1)/(\mathcal{F}(\rho_1) + \mathcal{F}(\rho_2))$ as a function of ρ_1 for $\rho_2 = 1$ and $\gamma = 1$. (a) Ψ given by the gamma distribution. (b) Ψ given by the Pareto-II distribution. We also set $\gamma = \kappa_0/D = 1$. Also shown is the splitting probability for totally absorbing targets ($\kappa_0 \rightarrow \infty$).

the splitting probabilities and MFPTs for more than one target.

For the sake of illustration, consider two spherical targets of rescaled radii ρ_1 and ρ_2 such that ρ_2 is fixed at unity. In Fig. 4 we plot the leading-order contribution to the splitting probability π_1 of the first target, see Eq. (5.1), as a function of the target radius ρ_1 for the gamma and Pareto-II models. As expected, $\pi_1 = 0.5$ when $\rho_1 = \rho_2 = 1$. In the case of the gamma model, π_1 is a sigmoid-like function of ρ_1 whose steepness increases significantly with the α -coefficient. That is, for large α , small changes in ρ_1 leads to large changes in the renormalized radius, and thus the splitting probability π_1 . The latter effect is much weaker in the case of the Pareto-II model. In Fig. 5 we show corresponding plots of the leading-order contribution to the conditional MFPT of the first target, T_1 . (In fact, Eq. (5.2) implies that at $O(1/\epsilon)$, $T_j \propto 1/\sum_k \mathcal{F}(\rho_k)$ for all $j = 1, \dots, N$.) In contrast to the splitting probability, T_1 is sensitive to the choice of α for both models. As might be expected, the MFPT is increased relative to the case of totally absorbing targets ($\kappa_0 \rightarrow \infty$) due to the renormalization of the target sizes.

VI. DISCUSSION

In this paper we analyzed the 3D narrow capture problem for small spherical targets with partially reactive boundary surfaces. We proceeded by combining matched asymptotic analysis with an encounter-based formulation of diffusion-mediated surface reactions. In particular, we derived an asymptotic expansion of the joint probability density (propagator) for the position and boundary local

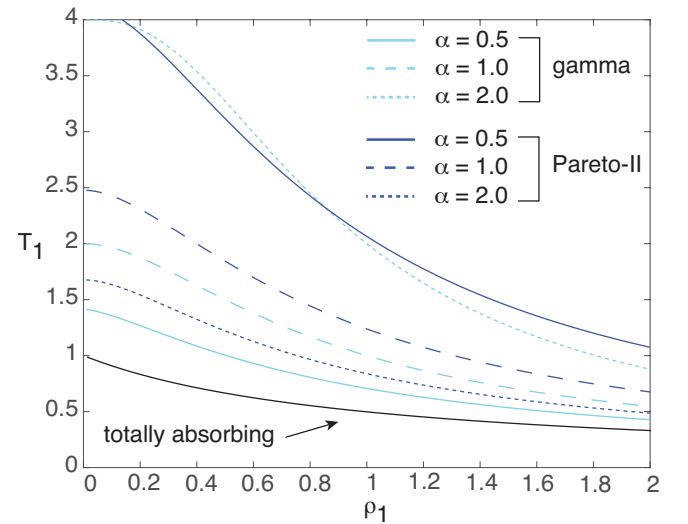


FIG. 5. Two spherical targets with rescaled radii ρ_1 and ρ_2 . Plot of leading-order contribution to the non-dimensionalized conditional MFPT of the first target, $T_1 \sim 1/(\mathcal{F}(\rho_1) + \mathcal{F}(\rho_2))$ as a function of ρ_1 for fixed $\rho_2 = 1$ and $\gamma = 1$. Also shown is the splitting probability for totally absorbing targets ($\kappa_0 \rightarrow \infty$).

time of reflected Brownian motion. The effects of surface reactions were then incorporated via an appropriate stopping condition for the boundary local time. We illustrated the theory by investigating how surface reactions affected the splitting probabilities and conditional mean FPTs. We showed that to leading order there is an effective renormalization of the target radius of the form $\rho \rightarrow \rho - \tilde{\Psi}(1/\rho)$, where $\tilde{\Psi}$ is the Laplace transform of the

stopping local time distribution. Moreover, in the case of an exponential law, we recovered the results of classical Robin boundary conditions. On the other hand, details regarding target positions and the geometry of the bulk domain only appear at higher orders.

In order to facilitate the analysis, we made two major simplifying assumptions. First, we considered spherically-shaped targets. However, as originally shown by Ward and Keller [1, 2], it is possible to generalize the asymptotic analysis of narrow capture problems to more general target shapes such as ellipsoids by applying classical results from electrostatics. In the case of totally absorbing targets one simply replaces the target length ρ_j in the far-field behavior of the inner solution by the capacitance C_j of an equivalent charged conductor with the shape \mathcal{U}_j . In addition, using the divergence theorem, it can then be shown that the flux into a target is completely determined by the far-field behavior. However, the analysis is considerably more complicated when considering partially reacting target surfaces. In particular, one has to consider multipole contributions to the inner solutions. The second major assumption was to take the rule for surface reactions to be the same for each target, which meant that we only needed to keep track of a single boundary local time. If each target were to have a different probability distribution for the stopping local time, then it would be necessary to introduce multiple local times ℓ_j , $j = 1, \dots, N$ [45]. The associated propagator would then be $P = P(\mathbf{x}, \ell_1, \dots, \ell_N, t | \mathbf{x}_0)$ such that the marginal probability density becomes

$$p(\mathbf{x}, t | \mathbf{x}_0) = \int_0^\infty d\ell_1 \Psi_1(\ell_1) \dots \int_0^\infty d\ell_N \Psi_N(\ell_N) \times P(\mathbf{x}, \ell_1, \dots, \ell_N, t | \mathbf{x}_0).$$

Calculating the propagator is significantly more involved.

Finally, note that a complementary approach to dealing with partially reactive surfaces arises within the context of multi-scale computational models of reaction-diffusion (RD) systems. A major challenge in simulating intracellular processes is how to efficiently couple stochastic chemical reactions involving low molecular numbers with diffusion in complex environments. One approach is to consider a spatial extension of the Gillespie algorithm for well-mixed chemical reactions [46, 47] using a mesoscopic compartment-based method, although there are subtle issues with regards choosing the appropriate compartment size [48–51]. Alternatively, one can combine a coarse-grained deterministic RD model in the bulk of the domain with individual particle-based Brownian dynamics in certain restricted regions [52–55]; in this case considerable care must be taken in the choice of boundary conditions at the interface between the two domains. This is somewhat analogous to having to deal with boundary local times in partially reflecting Brownian motion.

APPENDIX A. DERIVATION OF THE PROPAGATOR BVP USING A FEYNMAN-KAC FORMULA

Another way to define the propagator $P(\mathbf{x}, \ell, t | \mathbf{x}_0)$ introduced in Sect. III is in terms of the expectation of a Dirac delta function with respect to the distribution of paths between $(\mathbf{x}_0, 0)$ to (\mathbf{x}, t) :

$$P(\mathbf{x}, \ell, t | \mathbf{x}_0) = \left\langle \delta(\ell - D\mathcal{T}(\partial\Omega, t)) \right\rangle_{\mathbf{x}_0=\mathbf{x}_0}^{\mathbf{x}_t=\mathbf{x}}, \quad (\text{A.1})$$

where

$$\mathcal{T}(\partial\Omega, t) = \int_0^t \int_{\partial\Omega} \delta(\mathbf{X}_\tau - \mathbf{x}) d\mathbf{x} d\tau. \quad (\text{A.2})$$

That is, the joint probability density is obtained by summing over all paths whose accumulative boundary local time is equal to ℓ . Using a Fourier representation of the Dirac delta function, Eq. (A.1) can be rewritten as

$$P(\mathbf{x}, \ell, t | \mathbf{x}_0) = \int_{-\infty}^{\infty} e^{i\omega\ell} \mathcal{G}(\mathbf{x}, \omega, t | \mathbf{x}_0) \frac{d\omega}{2\pi}, \quad (\text{A.3})$$

where $P(\mathbf{x}, \ell, t | \mathbf{x}_0) = 0$ for $\ell < 0$ and

$$\mathcal{G}(\mathbf{x}, \omega, t | \mathbf{x}_0) = \left\langle \exp(-i\omega D\mathcal{T}(\partial\Omega, t)) \right\rangle_{\mathbf{x}_0=\mathbf{x}_0}^{\mathbf{x}_t=\mathbf{x}}. \quad (\text{A.4})$$

We now note that \mathcal{G} is the characteristic functional of the Brownian local time, which can be evaluated using a path-integral representation of the stochastic process. The latter can then be used to derive the following Feynman-Kac equation [56, 57]:

$$\frac{\partial \mathcal{G}(\mathbf{x}, \omega, t | \mathbf{x}_0)}{\partial t} = D\nabla^2 \mathcal{G}(\mathbf{x}, \omega, t | \mathbf{x}_0) - i\omega D \int_{\partial\Omega} \mathcal{G}(\mathbf{x}', \omega, t | \mathbf{x}_0) \delta(\mathbf{x} - \mathbf{x}') d\mathbf{x}'. \quad (\text{A.5})$$

Multiplying Eq. (A.5) by $e^{i\omega\ell}$, integrating with respect to ω and using the identity

$$\frac{\partial}{\partial \ell} P(\mathbf{x}, \ell, t | \mathbf{x}_0) \Theta(\ell) = \int_{-\infty}^{\infty} i\omega D e^{i\omega\ell} \mathcal{G}(\mathbf{x}, \omega, t | \mathbf{x}_0) \frac{d\omega}{2\pi},$$

with $\Theta(\ell)$ the Heaviside function, we obtain the result

$$\begin{aligned} \frac{\partial P(\mathbf{x}, \ell, t | \mathbf{x}_0)}{\partial t} &= D\nabla^2 P(\mathbf{x}, \ell, t | \mathbf{x}_0) \\ &\quad - D \int_{\partial\Omega} \frac{\partial P}{\partial \ell}(\mathbf{x}', \ell, t | \mathbf{x}_0) \delta(\mathbf{x} - \mathbf{x}') d\mathbf{x}' \\ &\quad - D\delta(\ell) \int_{\partial\Omega} P(\mathbf{x}', 0, t | \mathbf{x}_0) \delta(\mathbf{x} - \mathbf{x}') d\mathbf{x}'. \end{aligned} \quad (\text{A.6})$$

This is equivalent to the BVP

$$\begin{aligned} \frac{\partial P(\mathbf{x}, \ell, t | \mathbf{x}_0)}{\partial t} &= D\nabla^2 P(\mathbf{x}, \ell, t | \mathbf{x}_0), \quad \mathbf{x} \in \Omega \\ - D\nabla P(\mathbf{x}, \ell, t | \mathbf{x}_0) \cdot \mathbf{n} &= DP(\mathbf{x}, \ell = 0, t | \mathbf{x}_0) \delta(\ell) \\ + D \frac{\partial}{\partial \ell} P(\mathbf{x}, \ell, t | \mathbf{x}_0), \quad &\mathbf{x} \in \partial\Omega, \end{aligned}$$

which reduces to Eq. (3.11) on setting $P(\mathbf{x}, \ell = 0, t|\mathbf{x}_0) = -\nabla p_\infty(\mathbf{x}, t|\mathbf{x}_0) \cdot \mathbf{n}$ for $\mathbf{x} \in \partial\Omega$. The latter equality can be understood by noting that a constant reactivity is equivalent to a Robin boundary condition. Thus

$$\begin{aligned} \nabla p(\mathbf{x}, t|\mathbf{x}_0) \cdot \mathbf{n} &= -\kappa p(\mathbf{x}, t|\mathbf{x}_0) \\ &= -\kappa \int_0^\infty e^{-\kappa\ell} P(\mathbf{x}, \ell, t|\mathbf{x}_0) d\ell. \end{aligned} \quad (\text{A.7})$$

The result follows from taking the limit $\kappa \rightarrow \infty$ on both sides and noting that $\lim_{\kappa \rightarrow \infty} \kappa e^{-\kappa\ell}$ is the Dirac delta function on the positive half-line.

APPENDIX B. RECOVERY OF THE RESULTS FOR CONSTANT REACTIVITY

In this appendix we verify that Eqs. (4.25) and (4.26) for generalized surface reactions reduce to the results obtained for constant reactivity (Robin boundary conditions), which are given by Eqs. (2.13) and (2.22), respectively. First, setting $\Psi(\ell) = e^{-\gamma\ell}$ and $\tilde{\Psi}(q) = (q + \gamma)^{-1}$, we have

$$\begin{aligned} \tilde{q}_0^\Psi(\mathbf{y}, s|\mathbf{x}_0) &\rightarrow G(\mathbf{x}_j, s|\mathbf{x}_0) \left[1 - \frac{\rho_j}{|\mathbf{y}|} + \frac{1}{1 + \gamma\rho_j} \frac{\rho_j}{|\mathbf{y}|} \right] \\ &= G(\mathbf{x}_j, s|\mathbf{x}_0) \left[1 - \frac{\gamma\rho_j}{1 + \gamma\rho_j} \frac{\rho_j}{|\mathbf{y}|} \right] \\ &= G(\mathbf{x}_j, s|\mathbf{x}_0) \left[1 - \frac{\rho_j^\Lambda}{|\mathbf{y}|} \right] \end{aligned} \quad (\text{B.1})$$

which recovers Eq. (2.13). Second,

$$\chi_j^\Psi \rightarrow -4\pi D \sum_{k=1}^N G_{k0} \rho_k^\Lambda \mathcal{G}_{jk} = \chi_j^{(1)}(\Lambda),$$

see Eq. (2.17),

$$\begin{aligned} \frac{\tilde{\Psi}(1/\rho_k) - \tilde{\Psi}(1/\rho_j)}{\rho_j^{-1} - \rho_k^{-1}} - \rho_k \tilde{\Psi}(1/\rho_j) \\ \rightarrow -\frac{\rho_j \rho_k^2 \gamma}{(1 + \gamma\rho_j)(1 + \gamma\rho_k)}, \end{aligned}$$

and

$$\begin{aligned} g_j \rho_j \cos \theta &\left[\frac{|\mathbf{y}|}{\rho_j} - \frac{\rho_j^2}{|\mathbf{y}|^2} + \frac{3\rho_j \tilde{\Psi}(2/\rho_j)}{|\mathbf{y}|^2} \right] \\ &\rightarrow g_j \rho_j \cos \theta \left[\frac{|\mathbf{y}|}{\rho_j} + \frac{\rho_j^2}{|\mathbf{y}|^2} \left(\frac{3}{2 + \gamma\rho_j} - 1 \right) \right] \\ &= g_j \rho_j \cos \theta \left[\frac{|\mathbf{y}|}{\rho_j} + \frac{\rho_j^2}{|\mathbf{y}|^2} \frac{1 - \gamma\rho_j}{2 + \gamma\rho_j} \right] = B_j^{(1)}(\mathbf{y}, \Lambda), \end{aligned}$$

see Eq. (2.21). Hence,

$$\begin{aligned} \tilde{q}_1^\Psi(\mathbf{y}, s|\mathbf{x}_0) &\rightarrow \chi_j^{(1)}(\Lambda) + B_j^{(1)}(\mathbf{y}, \Lambda) \\ &+ \frac{4\pi D}{|\mathbf{y}|} \sum_{k=1}^N G_{k0} \left\{ \frac{\rho_j \rho_k^2 \gamma}{1 + \gamma\rho_k} - \frac{\rho_j \rho_k^2 \gamma}{(1 + \gamma\rho_j)(1 + \gamma\rho_k)} \right\} \mathcal{G}_{jk} \\ &= \chi_j^{(1)}(\Lambda) + \frac{4\pi D}{|\mathbf{y}|} \sum_{k=1}^N G_{k0} \rho_j^\Lambda \rho_k^\Lambda \mathcal{G}_{jk} + B_j^{(1)}(\mathbf{y}, \Lambda) \\ &= \chi_j^{(1)}(\Lambda) \left(1 - \frac{\rho_j^\Lambda}{|\mathbf{y}|} \right) + B_j^{(1)}(\mathbf{y}, \Lambda) \end{aligned} \quad (\text{B.2})$$

and we recover Eq. (2.22).

[1] M. J. Ward and J. B. Keller, Strong localized perturbations of eigenvalue problems. *SIAM J Appl Math* **53** 770-798 (1993).

[2] M. J. Ward, W. D. Henshaw and J. B. Keller, Summing logarithmic expansions for singularly perturbed eigenvalue problems. *SIAM J. Appl. Math.* **53** 799-828 (1993).

[3] M. J. Ward, Diffusion and bifurcation problems in singularly perturbed domains. *Natural Resource Modeling* **13** (2000).

[4] R. Straube, M. J. Ward and M. Falcke, Reaction rate of small diffusing molecules on a cylindrical membrane. *J. Stat. Phys.* **129** 377-405 (2007).

[5] Z. Schuss, A. Singer and D. Holcman, The narrow escape problem for diffusion in cellular microdomains. *Proc. Natl. Acad. Sci. (U.S.A.)* **104** 16098 (2007).

[6] P. C. Bressloff, B. A. Earnshaw and M. J. Ward, Diffusion of protein receptors on a cylindrical dendritic membrane with partially absorbing targets. *SIAM J. Appl. Math.* **68** 1223-1246 (2008).

[7] O. Benichou and R. Voituriez Narrow escape time problem: Time needed for a particle to exit a confining domain through a small window. *Phys. Rev. Lett.* **100** 168105 (2008).

[8] D. Coombs, R. Straube and M. J. Ward, Diffusion on a sphere with localized targets: Mean first passage time, eigenvalue asymptotics, and Fekete points. *SIAM J. Appl. Math.* **70** 302-332 (2009).

[9] S. Pillay, M. J. Ward, A. Peirce, T. Kolokolnikov, An asymptotic analysis of the mean first passage time for narrow escape problems: Part I: Two-dimensional domains. *SIAM Multiscale Model. Sim.* **8** 803-835 (2010).

[10] J. Reingruber and D. Holman Narrow escape for a stochastically gated Brownian ligand. *J. Phys. Cond. Matter* **22** 065103 (2010).

[11] A. F. Cheviakov, M. J. Ward and R. Straube An asymptotic analysis of the mean first passage time for narrow

escape problems: Part II: The sphere. *SIAM J. Multiscale Mod. Sim.* **8** 836-870 (2010).

[12] A. F. Cheviakov and M. J. Ward Optimizing the principal eigenvalue of the Laplacian in a sphere with interior targets. *Math. Comp. Modeling* **53** 042118 (2011).

[13] C. Chevalier, O. Benichou, B. Meyer and R. Voituriez First-passage quantities of Brownian motion in a bounded domain with multiple targets: a unified approach. *J. Phys. A* **44** 025002 (2011).

[14] D. Holcman and Z. Schuss, The narrow escape problem *SIAM Rev.* **56** 213 (2014)

[15] V. Kurella, J. C. Tzou, D. Coombs and M. J. Ward, Asymptotic analysis of first passage time problems inspired by ecology. *Bull Math Biol.* **77** 83-125 (2015).

[16] M. I. Delgado, M. J. Ward and D. Coombs, Conditional mean first passage times to small targets in a 3-D domain with a sticky boundary: Applications to T cell searching behavior in lymph nodes. *Multiscale Model. Simul.* **13** 1224-1258 (2015)..

[17] P. C. Bressloff and S. D. Lawley, Stochastically-gated diffusion-limited reactions for a small target in a bounded domain. *Phys. Rev. E* **92** 062117 (2015).

[18] P. C. Bressloff and S. D. Lawley, Escape from subcellular domains with randomly switching boundaries. *Multiscale Model. Simul.* **13** 1420-1445 (2015).

[19] A. E. Lindsay , T. Kolokolnikov and J. C. Tzou, Narrow escape problem with a mixed target and the effect of orientation. *Phys. Rev. E* **91** 032111 (2015).

[20] A. E. Lindsay, R. T. Spoonmore and J. C. Tzou, Hybrid asymptotic-numerical approach for estimating first passage time densities of the two-dimensional narrow capture problem. *Phys. Rev. E* **94** 042418 (2016).

[21] A. E. Lindsay, A. J. Bernoff and M. J. Ward, First passage statistics for the capture of a Brownian particle by a structured spherical target with multiple surface targets. *Multiscale Model. Simul.* **15** 74-109 (2017).

[22] D. S. Grebenkov and G. Oshanin, Diffusive escape through a narrow opening: new insights into a classic problem. *Phys. Chem. Chem. Phys.* **19** 2723-2739 (2017).

[23] P. C. Bressloff, Asymptotic analysis of extended two-dimensional narrow capture problems. *Proc Roy. Soc. A* **477** 20200771 (2021).

[24] P. C. Bressloff, Asymptotic analysis of target fluxes in the three-dimensional narrow capture problem. *Multiscale Model. Simul.* **19** 612-632 (2021).

[25] P. C. Bressloff, Accumulation time of diffusion in a singularly perturbed domain. Preprint (2022).

[26] D. Holcman and Z. Schuss, *Stochastic Narrow Escape in Molecular and Cellular Biology* (Springer, New York, 2015).

[27] P. C. Bressloff, *Stochastic Processes in Cell Biology: Vols. I and II* (Springer 2022).

[28] S. A. Rice, Diffusion-limited reactions. (Elsevier, Amsterdam 1985).

[29] F. C. Collins and G. E. Kimball, Diffusion-controlled reaction rates. *J. Colloid Sci.* **4** 425-439 (1949).

[30] S. D. Lawley and J. P. Keener, A new derivation of Robin boundary conditions through homogenization of a stochastically switching boundary. *SIAM Journal on Applied Dynamical Systems* **14** 1845-1867 (2015).

[31] D. S. Grebenkov Imperfect Diffusion-Controlled Reactions. in *Chemical Kinetics: Beyond the Textbook*, Eds. K. Lindenberg, R. Metzler, and G. Oshanin (World Scientific, 2019).

[32] P. Lèvy Sur certaines processus stochastiques homogènes. *Compos. Math.* **7** 283 (1939).

[33] H. P. McKean Brownian local time. *Adv. Math.* **15** 91-111 (1975).

[34] M. Freidlin. *Functional Integration and Partial Differential Equations* Annals of Mathematics Studies (Princeton University Press, Princeton, New Jersey, 1985).

[35] V. G. Papanicolaou The probabilistic solution of the third boundary value problem for second order elliptic equations *Probab. Th. Rel. Fields* **87** 27-77 (1990).

[36] G. N. Milshtein The solving of boundary value problems by numerical integration of stochastic equations. *Math. Comp. Sim.* **38** 77-85 (1995).

[37] D. S. Grebenkov, M. Filoche, and B. Sapoval. Spectral Properties of the Brownian Self-Transport Operator. *Eur. Phys. J. B* **36** 221-231 (2003).

[38] D. S. Grebenkov. Partially reflected Brownian motion: A stochastic approach to transport phenomena. in *Focus on Probability Theory*, Ed. L. R. Velle, pp. 135-169 (Hauppauge: Nova Science Publishers, 2006).

[39] D. S. Grebenkov. Residence times and other functionals of reflected Brownian motion. *Phys. Rev. E* **041139** (2007).

[40] A. Singer, Z. Schuss, A. Osipov, and D. Holcman. Partially reflected diffusion. *SIAM J. Appl. Math.* **68** 844-868 (2008).

[41] D. S. Grebenkov Spectral theory of imperfect diffusion-controlled reactions on heterogeneous catalytic surfaces *J. Chem. Phys.* **151** 104108 (2019).

[42] D. S. Grebenkov Paradigm shift in diffusion-mediated surface phenomena. *Phys. Rev. Lett.* **125** 078102 (2020).

[43] D. S. Grebenkov An encounter-based approach for restricted diffusion with a gradient drift. arXiv:2110.12181 (2021).

[44] P. C. Bressloff, Diffusion-mediated surface reactions, Brownian functionals and the Feynman-Kac formula. Preprint (2022).

[45] D. S. Grebenkov, Joint distribution of multiple boundary local times and related first-passage time problems with multiple targets. *Journal of Statistical Mechanics: Theory and Experiment* **10** 103205 (2020).

[46] D. T. Gillespie, Exact stochastic simulation of coupled chemical reactions. *J. Phys. Chem.* **81** 2340-2361 (1977).

[47] D. T. Gillespie, Approximate accelerated stochastic simulation of chemically reacting systems. *J. Chem. Phys.* **115**,1716-1733 (2001).

[48] T. E. Turner, S. Schnell and K. Burrage, Stochastic approaches for modelling in vivo reactions. *Comp. Biol. Chem.* **28** 165-178 (2004).

[49] S. A. Isaacson and C. Peskin, Incorporating diffusion in complex geometries into stochastic chemical kinetics simulations, *SIAM J. Sci. Comp.* **28** 47-74 (2006).

[50] S. A. Isaacson, The reaction-diffusion master equation as an asymptotic approximation of diffusion to a small target. *SIAM J. Appl. Math.* **7** 77-111 (2009).

[51] J. Hu, H.-W. Kang and H. G. Othmer, Stochastic analysis of reaction-diffusion processes. *Bull. Math. Biol.* **76** 854-894 (2014)

[52] S. Andrews and D. Bray, Stochastic simulation of chemical reactions with spatial resolution and single molecule detail. *Phys. Biol.* **1** 137-151 (2004).

[53] R. Erban and S. J. Chapman, Reactive boundary conditions for stochastic simulations of reaction-diffusion processes. *Phys. Biol.* **4** 16-28 (2007).

- [54] R. Erban and S. J. Chapman, Stochastic modelling of reaction-diffusion processes: algorithms for bimolecular reactions. *Phys. Biol.* **6** 046001 (2009).
- [55] B. Franz, M. B. Flegg, S. J. Chapman and R. Erban, Multiscale reaction-diffusion algorithms: PDE-assisted Brownian dynamics. *SIAM J. Appl. Math.* **73** 1224-1247 (2013).
- [56] M. Kac, On distribution of certain Wiener functionals. *Trans. Am. Math. Soc.* **65**, 1-13 (1949).
- [57] S. N. Majumdar, Brownian functionals in physics and computer science. *Curr. Sci.* **89**, 2076 (2005).